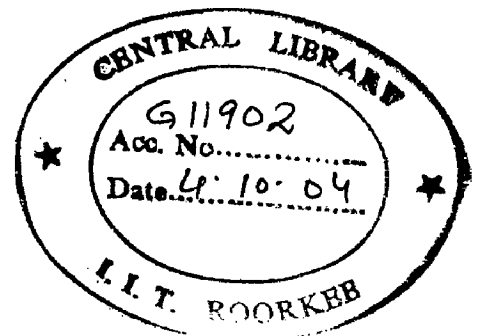


POWER SYSTEM STABILITY ENHANCEMENT USING PSS

A DISSERTATION

Submitted in partial fulfillment of the
requirements for the award of the degree
of
MASTER OF TECHNOLOGY
in
ELECTRICAL ENGINEERING
(With Specialization in Power System Engineering)

By
DINESH KUMAR



DEPARTMENT OF ELECTRICAL ENGINEERING
INDIAN INSTITUTE OF TECHNOLOGY ROORKEE
ROORKEE-247 667 (INDIA)

JUNE, 2004

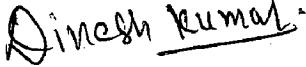
CANDIDATE'S DECLARATION

This is to certify that the report which is being presented in this dissertation titled “**Power System Stability Enhancement using PSS**” in partial fulfillment of the requirements for the award of the degree of **Master of Technology in Electrical Engineering**, with specialization in Power System Engineering, submitted in the department of **Electrical Engineering, Indian Institute of Technology, Roorkee** is an authentic record of my own work under the supervision of **Dr. Vinay Pant**, Assist. Professor, Electrical Engineering Department, Indian Institute of Technology, Roorkee and **Dr. B. Das** Assist. Professor, Electrical Engineering Department, Indian Institute of Technology, Roorkee.

I have not submitted the matter embodied in this report for the award of any other degree or diploma.

Date: 29-06-04

Place: Roorkee

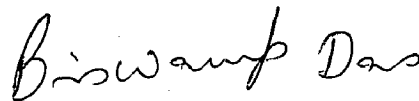

(DINESH KUMAR)

CERTIFICATE

This is to certify that the above statement made by the student is correct to the best of my knowledge.



(Dr. Vinay Pant)
Assistant Professor
Dept. of Electrical Engineering
Indian Institute of Technology, Roorkee



(Dr. B. Das)
Assistant Professor
Dept. of Electrical Engineering
Indian Institute of Technology, Roorkee

AKNOWLEDGEMENTS

I take this opportunity to express my deep sense of gratitude to both of my guides **Dr. Vinay Pant**, Assistant Professor, Department of Electrical Engineering Indian Institute of Technology Roorkee, Roorkee and **Dr. B.Das**, Assistant Professor, Department of Electrical Engineering, Indian Institute of Technology Roorkee, Roorkee for their continual guidance, constant encouragement, discussion and unceasing enthusiasm. I consider myself privileged to have worked under their guidance.

My heartfelt gratitude and indebtedness goes to **Dr. J. D. Sharma**, professor of Electrical Engineering Department, **Dr. Bharat Gupta**, Asst. Professor, O.C, PSS Lab for providing the necessary lab facilities. My sincere thanks to all **faculty** members of Power System Engineering for their constant encouraging and caring words, constructive criticism and suggestions, have contributed directly or indirectly in a significant way towards completion of this work.

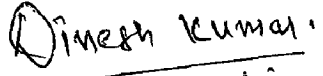
My heartfelt gratitude and deep respects are due to **Dr. Ramnarayan Patel**, who has been constant source of inspiration and encouragement for me during this work.

I am thankful to all research scholars of Power System Engineering, especially **Mr. Ashwani Kumar** and **Mr. Dheeraj khatode** for their moral support, encouragement and timely help.

I am highly grateful to **Shri S. K. Kapoor** and **Shri Jai Pal Singh**, Lab. Technicians, Power System Simulation Lab. for providing the required facilities and cooperation during this work.

Last but not the least I am highly indebted to my **Parents**, **Family members** and all my **Friends** whose sincere prayers, best wishes, moral support and encouragement have a constant source of assurance, guidance, strength and inspiration to me.

Dated: 29-05-04


(Dinesh Kumar)

ABSTRACT

A new type of Power System Stabilizer based on fuzzy set theory is proposed to improve the dynamic performance of a single machine power system. To have good damping characteristic over a wide range of operating conditions, speed deviation ($\Delta\omega$) and acceleration ($\Delta\dot{\omega}$) of a machine are chosen as the input signals to the fuzzy stabilizer on the particular machine. These input signals are first characterized by a set of linguistic variables using fuzzy set notations. The fuzzy relation matrix, which gives the relationship between stabilizer inputs and stabilizer output, allows a set of fuzzy logic operations that are performed on stabilizer inputs to obtain the desired stabilizer output. The effect of variation of coordinates of triangular membership function and scaling factors on performance of FLPSS has been investigated.

The work also includes the dynamic stability of a machine connected to an infinite bus through a transmission line. K1-K6 model, as suggested by Heffron and Phillips, has been used to analyze the system dynamic stability. The effect of variation of loading conditions on K1-K6 parameters, effect of AVR gain on system stability has been studied. A systematic approach is introduced to tune the parameters of Delta-Omega PSS for single machine infinite bus system.

Work has also been carried out for a multimachine system. Identification of optimum locations for Power System Stabilizer using Participation factor and Sensitivity methods. Then the multimachine system is simulated with Conventional Power System Stabilizer. All these work has been done using MATLAB 6.5 Simulink Tools.

CONTENTS

	Page No.
CANDIDATE DECLARATION	i
ACKNOWLEDGEMENT	ii
ABSTRACT	iii
LIST OF FIGURES	iv-vi
Chapter-1 Introduction	1-6
1.1 General	1
1.2 Review of literature	2
1.3 Outline of Dissertation work	5
Chapter -2 PSS for SMIB System	7-23
2.1 Introduction	7
2.2 Fuzzy Logic PSS for SMIB system.	8
2.3 System Investigated	8
2.4 Dynamic Model of the System in State Space Form	9
2.5 Fuzzy Logic PSS	13
2.6 Analysis	18
Chapter -3 Delta-Omega PSS for SMIB System.	24-40
3.1 Introduction	24
3.2 System Investigated	26
3.3 Small perturbation model transfer function model	26
3.4 Dynamic model in state space form of a SMIB system with AVR	27
3.5 To study the effect of system loading on K1-K6 parameters.	30
3.6 Effect of AVR gain	30
3.7 Dynamic model in state space form of a SMIB system with Delta - Omega PSS	30
3.8 Design of Robust Delta-Omega PSS	31
3.9 Dynamic performance of the system	33
3.10 Sensitivity analysis of the system	39
3.10.1 Effect of variation in real Power P	39
3.10.2 Effect of variation in reactive power Q	39
3.10.3 Effect of variation in transmission line reactance Xe.	39
3.10.4 Effect of variation in inertia constant H.	39
3.11 Conclusion.	40
Chapter-4 Identification of Optimum Location for PSS	41-47
4.1 Introduction	41
4.2 Methods of PSS location	42
4.3 Optimum PSS site	45
4.4 Optimum Location of PSS for Multi -Machine System	45
Chapter-5 PSS for Multi-Machine System	48-65
5.1 Introduction	48
5.2 Illustrative System Example	48
5.3 System Modeling	
5.3.1 Mathematical Modelling of the System.	49
5.3.2 Simulink Models.	51
5.4 Simulation Result.	51

Chapter-6 Conclusion and Scope for Further Work	Page No.
6.1 Conclusion	66-67
6.2 Scope for Further Work.	66
	67
REFERENCES	I-III
APPENDIX	a-k
APPENDIX 3.1	a
APPENDIX 3.2	b
APPENDIX 3.3	c-d
APPENDIX 3.4	e-f
APPENDIX 3.5	g-h
APPENDIX 5.1	i-j
APPENDIX 5.2	k
NOMENCLATURE	1-4

LIST OF FIGURE

- 2.1 Signal Machine with Infinite Bus System.
- 2.2 System Model without PSS.
- 2.3(a) System Model with CPSS.
- 2.3(b) Internal model of CPSS.
- 2.4. Triangular membership function.
- 2.5. Decision Table.
- 2.6. System Model with FLPSS.
- 2.7. Variation of speed deviation with time.
- 2.8. Variation of rotor angle with time.
- 2.9. Variation in the coordinates of the membership function.
- 2.10. Variation of speed deviation with time after changing the coordinates of the membership function.
- 2.11. Variation of rotor angle deviation with time after changing the coordinates of the membership function.
- 3.1 Block Diagram representation of SMIB system with AVR.
- 3.2 Block Diagram representation of SMIB system Delta-Omega PSS.
- 3.3 The variation of parameters (K1-K6) with variation in system load.
- 3.4 Delta-Omega Power System Stabilizer.
- 3.5(a) Dynamic Response without PSS, Rotor speed variation for $\Delta T_m = 0.05$ p.u.
- 3.5(b) Dynamic response without PSS, Rotor angle variation for $\Delta T_m = 0.05$ p.u.
- 3.6(a) Dynamic response with PSS, Rotor speed variation for $\Delta T_m = 0.05$ p.u.
- 3.6(b) Dynamic response with PSS, Rotor angle Variation for $\Delta T_m = 0.05$ p.u.
- 3.6(c) Dynamic response with PSS, Terminal Power Variation for $\Delta T_m = 0.05$ p.u.
- 3.6(d) Dynamic response with PSS, Terminal Voltage variation for $\Delta T_m = 0.05$ p.u.
- 3.6(e) Dynamic response with PSS, Rotor speed variation for $\Delta T_m = 0.05$ p.u.

- 3.7 Dynamic response with PSS, Rotor speed variation for $\Delta T_m = 0.05$ p.u. & different value External Reactance (0.2 p.u. to 0.9 p.u.).
- 3.8 Dynamic response with PSS, Rotor speed variation for $\Delta T_m = 0.05$ p.u. & different value Inertia Constant.
- 4.1 WSCC 3-machine, 9-bus system.
 - 5.1(a) Angular position of individual generators when FCT=0.1 sec.
 - 5.1(b) Relative angular positions δ_{21} and δ_{31} when FCT=0.1 sec.
 - 5.1(c) Relative angular velocities ω_{21} and ω_{31} when FCT=0.1 sec.
 - 5.1(d) Generator accelerating powers when FCT=0.1 sec
 - 5.2(a) Relative angular positions δ_{21} and δ_{31} when FCT=0.16 sec.
 - 5.2(b) Relative angular velocities ω_{21} and ω_{31} when FCT=0.16 sec.
 - 5.2(c) Generator accelerating powers when FCT=0.16 sec
 - 5.3(a) Relative angular positions δ_{21} and δ_{31} when FCT=0.17 sec.
 - 5.3(b) Relative angular velocities ω_{21} and ω_{31} when FCT=0.17 sec.
 - 5.3(c) Generator accelerating powers when FCT=0.17 sec
 - 5.4(a) Relative angular velocities ω_{21} with FCT=0.1 sec.
 - 5.4(b) Relative angular velocities ω_{23} with FCT=0.1 sec.
 - 5.4(c) Generator accelerating powers #1 with FCT=0.1 sec.
 - 5.4(d) Generator Accelerating Power #2 with FCT=0.1 sec.
 - 5.4(e) Generator Accelerating Power #3 with FCT=0.1 sec.
 - 5.5(a) Relative angular velocities ω_{21} with FCT=0.16 sec.
 - 5.5(b) Relative angular velocities ω_{23} with FCT=0.16 sec.
 - 5.5(c) Generator accelerating powers #1 with FCT=0.16 sec.
 - 5.5(d) Generator Accelerating Power #2 with FCT=0.16 sec.
 - 5.5(e) Generator Accelerating Power #3 with FCT=0.16 sec.
 - 5.6(a) Relative angular velocities ω_{21} with FCT=0.17 sec.
 - 5.6(b) Relative angular velocities ω_{23} with FCT=0.17 sec.

- 5.6(c) Generator accelerating powers #1 with FCT=0.17 sec.
- 5.6(d) Generator Accelerating Power #2 with FCT=0.17 sec.
- 5.6(e) Generator Accelerating Power #3 with FCT=0.17 sec.

1.1 General

Small signal stability is the ability of the power system to maintain synchronism under small perturbations. The small signal dynamic stability of electric power system has been the subject of major theoretical and practical interest and it continues to grow in importance as the control requirements of the power plants become more sophisticated and demanding.

The disturbances occur continually in a power system because of variations in the load and generation. The disturbances are considered sufficiently small for linearization of system equations to be permissible, for purposes of analysis. Small signal instability that may result can be of two forms.

- (i) Steady increase in rotor angle due to lack of sufficient synchronizing torque.
- (ii) Rotor oscillations of increasing amplitude due to lack of sufficient damping torque.

The low frequency rotor oscillations, also called the electromechanical models are in the range of 0.2 to 2.5 Hz. The damping characteristics of synchronous machine's rotor oscillations is a function of system structures, operating condition and control structures. The power system stabilizers are widely used to damp out low frequency oscillations. Eigen value analysis has become the main tool for the study of this type of power system stability problem.

In many cases, the system is approximated for design purposes by single machine tied to an infinite bus, which cannot reflect the interaction between machines e.g. inter area modes. As such a linear model of multimachine system is sought which does less approximation and more or less replicates the actual system.

Also, the optimum application of stabilizer is well defined and straightforward in cases where the instability is clearly identified with a machine or a group of machines. However, in more general case of widespread oscillation permeating a large

interconnection, the identification of optimum sites for stabilizer application is complicated. To be effective the stabilizer must be applied to machine that is both near antinodes of the slightly damped modes of oscillations and connected via low enough transfer impedances to induce strong damping torque in the surrounding machines. Experience with the stabilizer application is rapidly developing but geographically loose interconnections have shown that the straight forward course of applying stabilizers at all new plants can be ineffective because these machines are not necessarily located at best points for damping of troublesome modes of oscillations.

Hence, in view of the potentially high costs of applying stabilizers to older machines, it is vital that the relative effectiveness of stabilizers at all system locations be studied and PSS be applied or provided at all new machines and retrofitted only to those older machines where they are essential for satisfactory system damping.

1.2 Review of Literature

Over the last few decades, a large number of research papers have appeared in the area of power system stabilizers. A brief review of the relevant research work is being made in this section.

Kundur. et. al [1] provide a general introduction to the power system stability problem, including a discussion of the basic concepts, classification, and the definitions of related terms. This also includes the basic block diagram of the Power System Stabilizer.

Padiyar . et. al [2] provide the basic concepts in applying, design and application of Power System Stabilizer .it also include the control signals , recent development and future trends of the Power System Stabilizer.

M.A.Pai . et . al [4] provide the basic approach, derivation of K1-K6 constants, synchronizing and damping torques. It also includes the Power System Stabilizer design.

Kundur et. al [5] has described a procedure for the design of power system stabilizer for a major generating station in Ontario. They have considered two alternative control schemes, one with and other with out transient gain reduction (TGR). Their investigations revel that, with appropriate selection of stabilizer parameters, both schemes provide satisfactory overall performance. They have also reported the importance of appropriate choice of wash out time constant and stabilizer limits in addition to phase lead compensation circuit parameters.

Lee et. al [6] have further analyzed the performance of a power system stabilizer using speed and electrical power input as originally suggested by De Mello et. al. [8]. They have presented the design, testing and commissioning of this type of stabilizers on large fossil fired and nuclear units.

El-Metwally and Malik at. al [7] has proposed a Fuzzy Logic Power System Stabilizer (FLPSS) with speed deviation ($\Delta\omega$) and active power deviation (ΔPe) as inputs to FLPSS considering seven linguistic variables and triangular membership function. They also have considered center of gravity (COG) defuzzifier.

Y.Zhang et. al [9] has proposed an Artificial neural network (ANN) based power system stabilizer and its application to power system. The ANN based PSS combines the advantages of self- optimizing pole shifting adaptive control strategy and the quick response of ANN to introduce a new generation PSS. A popular type of ANN, the multi-layer perception with error back propagation training method, is employed in this PSS .the ANN was trained by the training data group generated by the adaptive power system stabilizer (APSS). During the training, the ANN was required to memorize and simulate the control strategy of APSS until the differences are within the specified criteria.

Y.L.Abdel et. al [10] has proposed an optimal multiobjective design of robust multimachine power system stabilizer(PSS) using genetic algorithms. A conventional speed- based lead-lag PSS is used in this work. The multimachine power system operating at various loading conditions and system configurations is treated as a finite set

of plants. The stabilizers are tuned to simultaneously shift the lightly damped and undamped electromechanical modes of all plants to a prescribed zone in the s-plane

Heffron and Philips et. al [11] have analyzed the effect of amplifying voltage regulators on under excited operation of large synchronous generators. They were first to present small perturbation model of machine-infinite bus system. Their investigations reveals that the use of modern, continuous acting voltage regulators greatly increases the steady state stability limit of synchronous generator in the under excited region.

Larsen and Swans at. al [12] presented three-part paper entitled "Applying Power System Stabilizers". In first of the paper general concepts associated with applying PSS utilizing shaft speed, a.c. bus frequency and electric power inputs were presented. Second part of the paper discusses system performance criterion, tuning concepts, which enables attainment of these criterion and relative performance attainable with practical stabilizer equipment utilizing the three input signals. The third part discusses the practical considerations of tuning equipment in the field and equipment design, including minimizing the effects of torsional destabilization, power system noise.

Anderson [1], Kundur [2], and Yu [4] have presented a comprehensive analysis of small signal stability. The analysis presented develops a clear insight into the problems of modeling and application of PSS.

De Mello at. al [8] have stressed the importance of finding out the relative effectiveness of stabilizer at all system locations. They have proposed a method based on eigen vector analysis with which the effectiveness of stabilizer at a particular machine can be accurately determined. Arcidiacono et.al.[9] have also used the eigen value and eigen vector approach to locate the power system stabilizers.

Hiyama at. al [13] has presented a coherency based identification method for optimum siting of power system stabilizers. Decomposition of multimachine power

system into several coherent groups is done and the most effective selection of a generator to be equipped with a stabilizer in each coherent group is determined.

Lim et.al. [14] have given a method for designing decentralized stabilizers by determine the parameters of all stabilizers in the system such that some or all of its mechanical mode eigen values have desired locations in the complex plane.

Hsu and Chen et. al [15] have proposed a novel approach for finding optimum locations for stabilizer using participation factors. The proposed method is found to be convenient for identification of stabilizer location because the participation factors are real numbers and easy to compute.

E.Z.Zhat et. al [16] has used the concept of participation factors and extended it by introducing new coupling factors where application of stabilizer yields maximum improvement of overall system damping characteristics.

Chern-Lin Chen et.al. [17] have proposed a technique for siting of power system stabilizers in a multimachine system by way of eigen value sensitivity model analysis.

HSU Y.Y et.al [18] have proposed the participation method for optimum location of PSS in multimachine system.

The research work pertaining to application of power system stabilizers to a multimachine system shows that identification of troublesome modes and location of power system stabilizers plays a very significant role for designing optimum power system stabilizers.

1.3 Outline of the Dissertation Work:

Chapter-1: Presents the brief review of the problem of small signal stability. This also includes the literature review of FLPSS, Delta-Omega PSS, Optimal location and PSS for multimachine system.

Chapter-2: Presents the designing an FLPSS with the help of MATLAB/Simulink. The coordinates of the triangular membership functions have been optimized. It also presents a comparison of system performance of an optimal conventional PSS with that with FLPSS.

Chapter-3: Presents the dynamic model of a single machine infinite bus system with IEEE type-I excitation system in state space form, with and without Delta-Omega PSS. Concepts of power system stability as affected by excitation system have been studied. A detailed sensitivity analysis of the system under varying loading conditions and system parameters has been carried out to understand the effect of these variations on dynamic performance.

Chapter-4: Presents a systematic approach for identifying the optimum location of Power System Stabilizer for a multimachine system using participation factor and sensitivity methods.

Chapter-5: Presents the stability analysis of a Multi machine system with the help of MATLAB/Simulink. This includes very popular model of multimachine system i.e. WSCC 3-machine, 9-bus system. In this result are compared with and without PSS.

Chapter-6: Present the conclusion and further work carried out in this dissertation. This chapter includes the summary of all the result of every chapter, which is carried out in this dissertation work.

2.1 Introduction

A lot of research work has been done in the past to find the ways and means to improve dynamic stability of a power system. Present trends in planning and operating of power system are to built power system with less redundancy and operate them closer to transient stability limit. So more reliance and emphasis is being placed on power system controls to provide required compensating effects to reduction in stability margins inherent from present day trends in system design. High gain excitation system equipped with power system stabilizer have been extensively used in modern power system as an effective means of enhancing overall power system stability.

With electric power systems, the change in electric torque of synchronous machine following a perturbation can be resolved in two components, i.e.

$$\Delta T_e = T_s \Delta \delta + T_d \Delta \omega$$

The component of torque change in phase with the rotor angle perturbation $\Delta \delta$ is referred as the synchronizing torque component and the component of torque in phase with the speed deviation $\Delta \omega$ is referred as the damping torque component. system stability depends on the existence of both components of torque for each of the synchronous machine.

The AVR gain plays a major role in system stability. The K1-K6 parameters vary with system loading. Hence magnitude and nature of synchronizing torque component and damping torque component depends on both system loading and AVR gain.

Tuning of supplementary excitation controls for stabilizing system modes of oscillations has been subject of much research. The basic tuning techniques utilized with PSS applications are phase compensation and root locus. To provide desired damping, stabilizer transfer function must compensate for the gain and phase characteristics of the excitation system, the generator and the power system, which collectively determine the stabilizer transfer function $GEP(s)$. It is also necessary to recognize the nonlinear nature

of power system. Hence it is a challenge to tune PSS to improve overall system stability over the wide operating range.

2.2 Fuzzy Logic PSS for SMIB System

A lot of work pertaining to Fuzzy Logic System Stabilizer (FLPSS) has been reported during the last few years. Critical review of the literature shows that most of the researchers have considered symmetrical triangular membership functions. No effort seems to have been made to study the effect of variation of co-ordinates of triangular membership functions on the performance of FLPSS. Moreover, COG defuzzification technique has invariably been used by most of the researcher. In view of the above the main objective of the work presented in this chapter are as follows.

1. To present an algorithm for designing FLPSS
2. To compare the dynamic performance of the FLPSS with a conventional PSS.
3. To study the effect of the variation of co-ordinates of the triangular membership functions on system dynamic performance and hence to obtain more or less optimum triangular membership functions.
4. To study the dynamic performance of the system considering several defuzzification techniques.

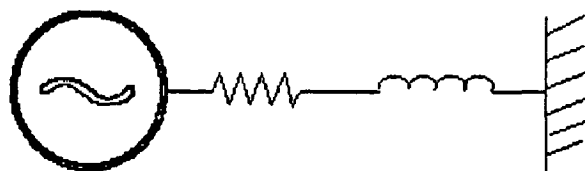


Fig 2.1. A Machine Infinite Bus

2.3 System Investigated

A machine infinite bus system is considered for analysis. Static excitation system is considered. Nominal parameters of the system are given below [2].

$L_{adu} = 1.65, L_{aqu} = 1.60, L_l = 0.16, Ra = 0.003, R_{fd} = 0.0006, L_{fd} = 0.153, R_E = 0.0, X_E$
 $= 0.65, K_A = 200, T_R = 0.02, K_{sd} = K_{sq} = 0.8491, i_{do} = 0.8342, i_{qo} = 0.4518, e_{do} = 0.6836, e_{qo}$
 $= 0.7298, K_{sd}(\text{iner}) = K_{sq}(\text{iner}) = 0.434, E_{ido} = 2.395, X_d = 1.81, X_q = 1.76, X'_d = 0.3, H$
 $= 3.5, K_d = 0, A_{sat} = 0.031, B_{sat} = 6.93, \psi_{\pi} = 0.8, W_0 = 377, K_{stab} = 9.5, T_w = 1.4, T_1 =$
 $0.154, T_2 = 0.033. \Delta v_s, \Delta \delta = 0.0873, \Delta \psi_{fd} = 0.2, \Delta v_1 = 0.1, \Delta v_2 = 0.1, \Delta v_s = 0.1$

Initial steady state conditions are taken as

$$P_t = 0.9, Q_t = 0.3, E_t = 1.0$$

2.4 Dynamic Model of the System in State Space Form

Following assumptions have been made in developing the dynamic model of the system.

1. The mechanical power input remains constant during the period of the transient.
2. Damping or a synchronous power is negligible.
3. The synchronous machine can be represented (electrically) by a constant voltage source behind a transient reactance.
4. The mechanical angle of the synchronous machine rotor coincides with the electrical phase angle of the voltage behind transient reactance.
5. If a local load is fed at the terminal voltage of the machine, it can be represented by a constant independence (or admittance) to neutral.

The non-linear model of the system is obtained as follows

$$\frac{d\omega}{dt} = \frac{(T_m - T_e)}{2H} \quad (2.1)$$

$$\frac{d\delta}{dt} = 2\pi f(\omega - \omega_0) \quad (2.2)$$

$$\frac{dv_1}{dt} = (E_t - V_1)/T_R \quad (2.3)$$

$$\frac{d\Psi_{fd}}{dt} = 2\pi f \left[R_{fd} \frac{E_{fd}}{L_{adu}} - R_{fd} L_{fd} \right] \quad (2.4)$$

a linear model of the system is obtained by linearizing the nonlinear model around a nominal operating point (transfer function model is given in the Fig. (2.2)).

The dynamic model of the linearized system in the state space form is obtained from the transfer function model in the form:

$$\dot{X} = AX + \Gamma p \quad (2.5)$$

$$\text{where } A = \begin{bmatrix} -\frac{K_D}{2H} & -\frac{K_1}{2H} & -\frac{K_2}{2H} & 0 \\ 2\pi f_0 & 0 & 0 & 0 \\ 0 & -\frac{K_3 K_4}{T_3} & -\frac{1}{T_3} & -\frac{K_3 K_A}{T_3} \\ 0 & -\frac{K_5}{T_R} & -\frac{K_6}{T_R} & -\frac{1}{T_R} \end{bmatrix}$$

$$X = \begin{bmatrix} \Delta\omega \\ \Delta\delta \\ \Delta\Psi_{fd} \\ \Delta v_1 \end{bmatrix}$$

$$\Gamma = \begin{bmatrix} 1 \\ 2H \\ 0 \\ 0 \\ 0 \end{bmatrix}$$

$$P = [\Delta T_m]$$

The eigen values of the closed loop system with PSS parameters

$K_{stab} = 9.5$, $T_1 = 0.154$, $T_2 = 0.033$ are shown below [2]

-39.0958; -1.0054+j6.6065; -1.0054+j6.6065; -0.7388; -19.7974-j12.8254;
-19.7974+j12.8254

Examine the eigen values of the system with conventional PSS it is clearly seen that for the typical values of the PSS parameters damping ratio for the electromechanical mode is 0.27

2.5 Fuzzy Logic PSS

2.5.1. Selection of Input Signals to Fuzzy Logic PSS

For the present investigations generators speed deviation ($\Delta\omega$) and acceleration ($\Delta\dot{\omega}$) are chosen as the input signals to the FLPSS.

In practice, only shaft speed deviation ($\Delta\omega$) is readily available. The acceleration ($\Delta\dot{\omega}$) is derived from the $\Delta\omega$ measured at two successive sampling instants

$$\Delta\dot{\omega} (KT) = \frac{\Delta\omega(KT) - \Delta\omega[(K-1)T]}{T}$$

Where T is the sampling period.

2.5.2 Selection of Linguistic Variables

The number of linguistic variables determines the quality of the control, which can be achieved using Fuzzy Logic Controllers. As the numbers of linguistic variables increases, the quality of control improves at the cost of increased computational time and computer memory. A compromise is needed between the two. For the power system under study, seven linguistic variables for each of the inputs and the output signals are considered. These seven linguistic variables are PB (positive big), NS (negative small), NM (negative medium) and NB (negative big). A choice of 7 linguistic variables results in a set of 49 "IF-THEN" rules (Fig. 2.5) shows the decision table. This table is obtained from the expert knowledge of the operators.

In order to obtain the minimum and the maximum values of the stabilizer inputs the dynamic performance of the system without PSS is obtained for different magnitudes of perturbations. After choosing the linguistic variables, it is required to determine the membership functions for these linguistic variables. Generally gaussian, triangular or trapezoidal membership functions are prevalent. Here triangular membership function is used to define the degree of membership (Fig. 2.4). Degree of membership plays a very important part in designing a fuzzy controller.

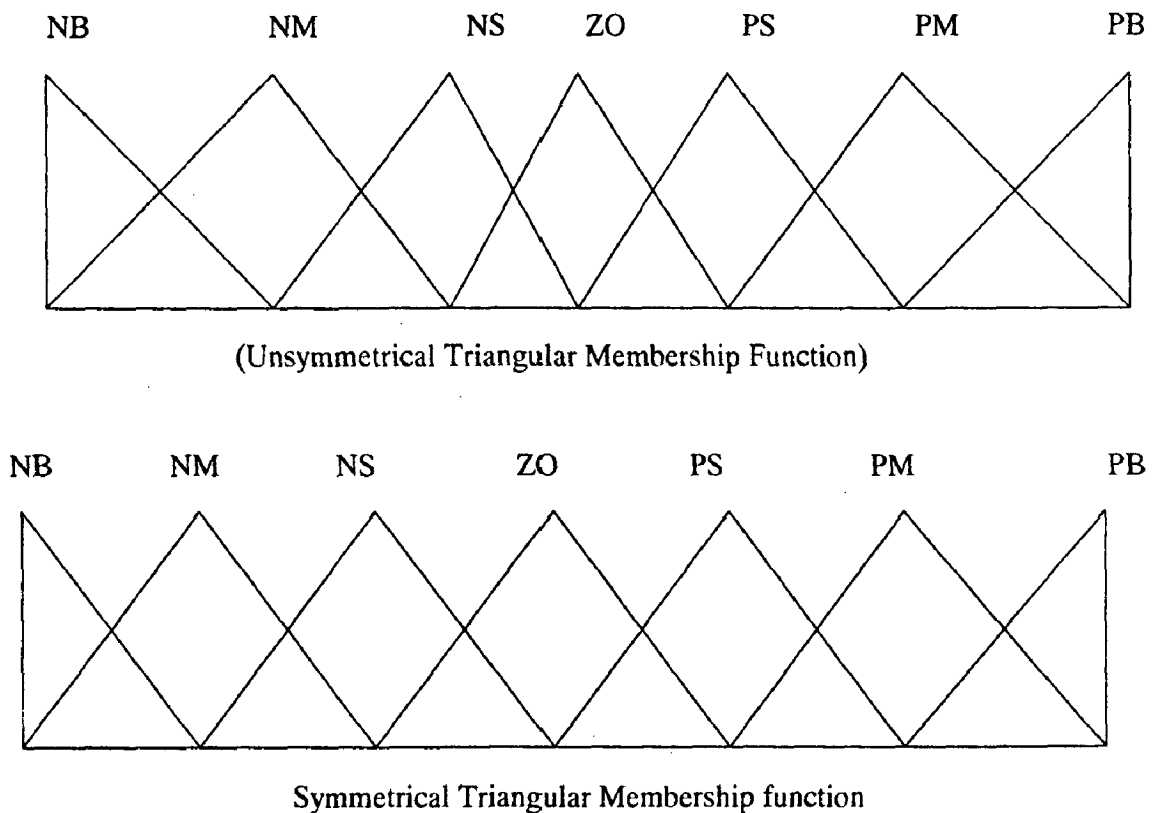


Fig. 2.4

Now it is required to find the fuzzy region for the output for each fuzzy rule, for which Madman implication is used.

Fuzzy rules are connected by AND operators and this operator are used to find the minimum between the two inputs membership functions. Later minimum between this result and the output membership function of a rule is calculated. This procedure is carried out for every rule and for every rule; an output membership function is obtained. To find the output membership function due to all these rules, the maximum among all of these rules is calculated. Suppose that at an arbitrary instant $\Delta\omega = -0.2$ and $\Delta\dot{\omega} = 1.3$.

$\Delta\dot{\omega}$	NB	NM	NS	ZO	PS	PM	PB
$\Delta\omega$							
NB	NB	NB	NB	NB	NM	NS	ZO
NM	NB	NB	NB	NM	NS	ZO	PS
NS	NB	NB	NM	NS	ZO	PS	PM
ZO	NB	NM	NS	ZO	PS	PM	PB
PS	NM	NS	ZO	PS	PM	PB	PB
PM	NS	ZO	PS	PM	PB	PB	PB
PB	ZO	PS	PM	PB	PB	PB	PB

Fig 2.5. Decision Table[7]

The input $\Delta\omega = -0.2$ corresponds to a linguistic variables NS and its membership function has a value of 0.2. It also belongs to the linguistic variable ZO with membership of 0.8. The fuzzy set for $\Delta\omega$ is defined as

$$\{\Delta\omega\} = \{(NB,0), (NM,0), (NS,0.2), (ZO,0.8), (PS,0), (PM,0), (PB,0)\}.$$

Similarly the second input $\Delta\dot{\omega} = 1.3$ corresponds to the linguistic variables PS and PM with memberships of 0.7 and 0.3 respectively. The fuzzy set for $\Delta\dot{\omega}$ becomes

$$\{\Delta\dot{\omega}\} = \{(NB, 0), (NM, 0), (NS, 0), (ZO, 0), (PS, 0.7), (PM, 0.3), (PB, 0)\}.$$

There is overlap between the membership functions corresponding to only two linguistic variables at any given instance. Any crisp input shall belong to two linguistic variables with a certain degree of membership. Since the controller has two inputs in total, we have $2 \times 2 = 4$ different combinations and so 4 rules shall be fired and corresponding to every rule there will be an output. Let $x_1, x_2, x_3,$ and x_4 be these outputs. The minimum operation on these 4 combinations results in membership functions.

$$\mu(x_1) = \mu(\Delta\omega \text{ is NS and } \Delta\dot{\omega} \text{ is PS})$$

$$\begin{aligned}
&= \min [\mu(\Delta\omega \text{ is NS}), \mu(\Delta\dot{\omega} \text{ is PS})] \\
&= \min [0.2, 0.7] \\
&= 0.2
\end{aligned}$$

From the table in the Fig 3.8 it is seen that when $\Delta\omega$ is NS and $\Delta\dot{\omega}$ is PS, then output y is ZO.

$$\begin{aligned}
\mu_y(\text{ZO}) &= \min[\mu(x_1), \mu(\text{ZO})] \\
&= \text{CLU}^1
\end{aligned}$$

CLU stands for the clipped value of U. the linguistic output = ZO is clipped at $\mu(x_1)=0.2$.

Similarly, when $\Delta\omega$ is NS and $\Delta\dot{\omega}$ is PM then output y is PS(CLU²). In the other two cases , the output y takes the linguistic values PM(CLU³) and PS(CLU⁴). CLU², CLU³ and CLU⁴ are calculated in a similar fashion. It is to be noted that CLU⁴=CLU² and therefore CLU⁴ may be neglected.

The fuzzy region is calculated by taking the cylindrical projection at every point.

Dynamic performance of the system with FLPSS is first examined considering the linear model. The same transfer function model as given in Fig2.3(a) with PSS block with $\Delta\omega$ as input.

The FLPSS operator in discrete mode. FLPSS output u is computed during each integrations step while solving the state equations using Rungta-Kutta technique. The dynamic model is with FLPSS is obtained from Fig. 2.6 as

$$\dot{X} = AX + Bu + \Gamma p$$

$$\text{Where } A = \begin{bmatrix} -\frac{K_D}{2H} & -\frac{K_1}{2H} & -\frac{K_2}{2H} & 0 \\ 2\pi f_0 & 0 & 0 & 0 \\ 0 & -\frac{K_3K_4}{T_3} & \frac{1}{T_3} & -\frac{K_3K_A}{T_3} \\ 0 & -\frac{K_5}{T_R} & K_6T_R & 0 \end{bmatrix}$$

2.6 Analysis

Following studies have been carried out considering Fuzzy Logic Power System Stabilizers.

1. Comparisons of the transient performance of the system with conventional PSS and FLPSS.
2. Effect of variation of co-ordinates of triangular membership function.
3. Effect of different alternative defuzzification techniques.

2.6.1 Comparison of Dynamic Performance of the System with Conventional PSS and FLPSS

Fig. 2.7 and 2.8 shows the transient response for $\Delta\omega$ and $\Delta\delta$ respectively following a 5 % step change in mechanical torque with conventional PSS and FLPSS obtained considering a linear model of the system. The scaling factors for $\Delta\omega$ and $\Delta\delta$ the stabilizing signals are respectively 5000, 350 and 500. Examination of the responses clearly shows that dynamic performance of the system with FLPSS is very close to that with conventional PSS and is in fact slightly better in terms of settling time. Further, in order to compare the dynamic performances quantitatively a quadratic performance index

$$J = \int_0^{\infty} [\Delta\omega(t)]^2 dt = \sum_{k=0}^{\infty} [\Delta\omega(kt)]^2 \Delta t \quad \text{is evaluated.}$$

Table 3.1 shows the value of J for CPSS and FLPSS. it also shows the peak overshoot of the dynamic response for $\Delta\omega$ and $\Delta\delta$. COG defuzzifier has been used and symmetrical triangular membership functions with equal base widths have been considered.

Type of PSS	J	Setting Time (Sec.)		Peak Overshoot	
		$\Delta\omega$	$\Delta\delta$	$\Delta\omega$	$\Delta\delta$
Conventional PSS	3.517×10^{-7}	3.7	3.7	0.024	2.7
FLPSS	2.217×10^{-7}	3.0	3.0	0.021	2.4

Table 2.1

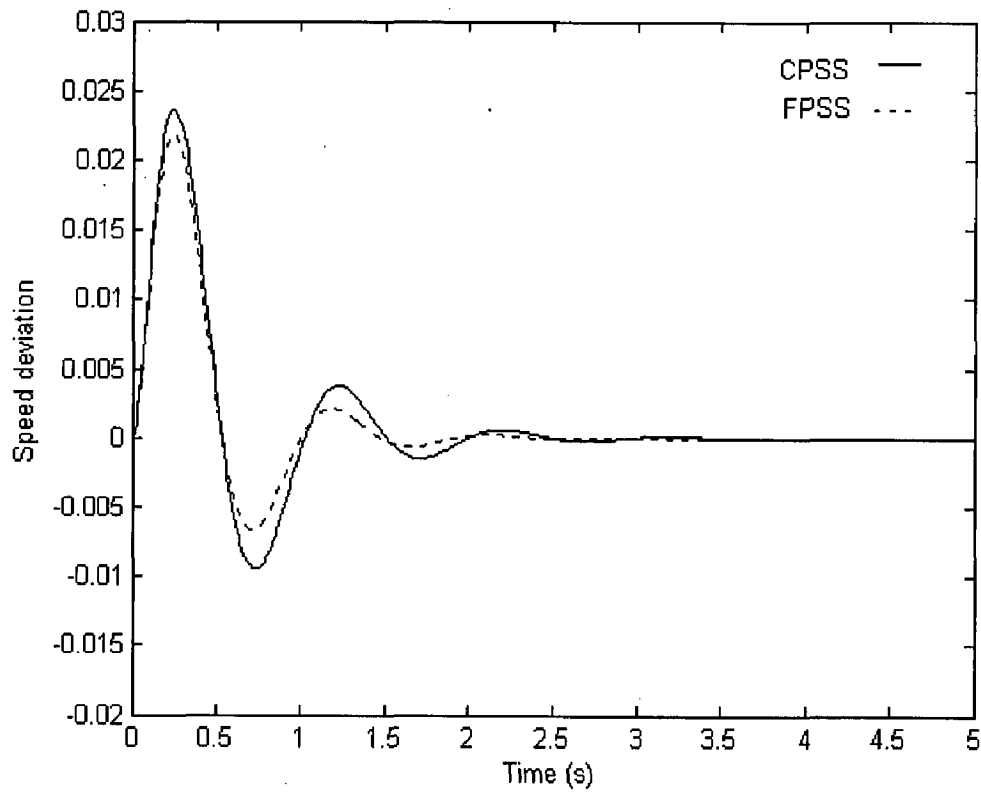


Fig. 2.7 Variation of speed deviation with time.

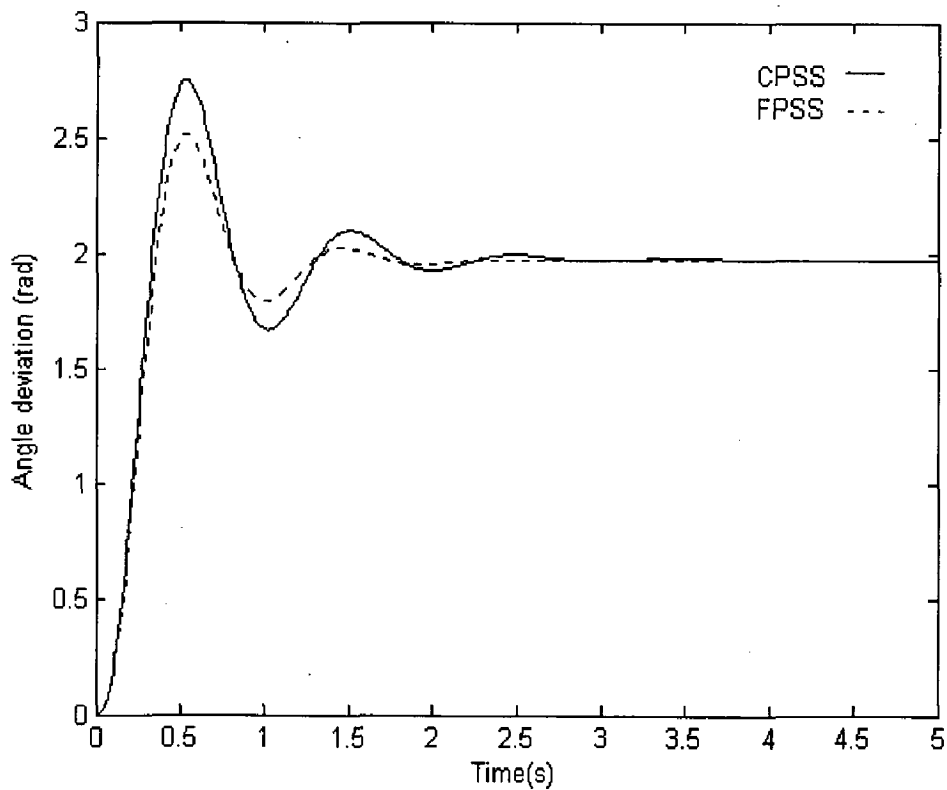


Fig. 2.8 Variation of speed deviation with time.

It is clearly that J obtained with FLPSS hardly differs from that with conventional PSS, whereas the peak overshoot also remains almost the same. However, the settling time falls by nearly 25%.

2.6.2 Effect of Variation of Coordinates of Triangular Membership

Function:

An attempt has been made towards gain tuning of the fuzzy logic controller by altering the coordinates of the membership functions. Centre of Gravity / Area (COG/COA) defuzzifier is used in the analysis.

Fig.2.9 (a) shows a triangular membership functions, α, β, γ are the coordinates of the function. α denotes the left coordinate of the base β denotes the abscissa of the peak and γ denotes the right coordinate of the base. Let β_1, β_2 and β_3 be the x coordinates of the peaks of the membership functions PS, PM and PB respectively.

For the membership functions PS let $c_1 = \beta_1$

For the membership functions PM let $y = \beta_2 - \beta_1$

For the membership functions PB let $z = \beta_3 - (\beta_1 + \beta_2)$
 $= 3 - (y + c_1)$

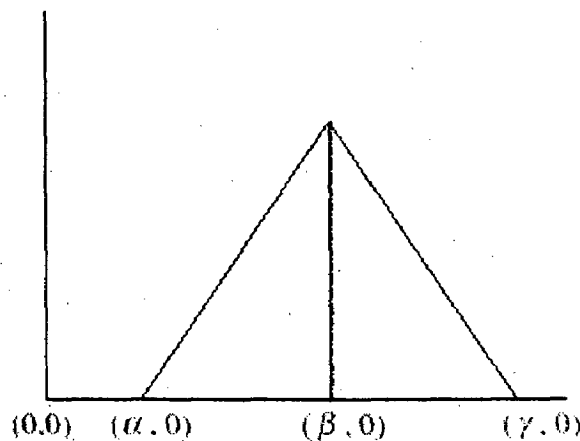


Fig. 2.9 (a)

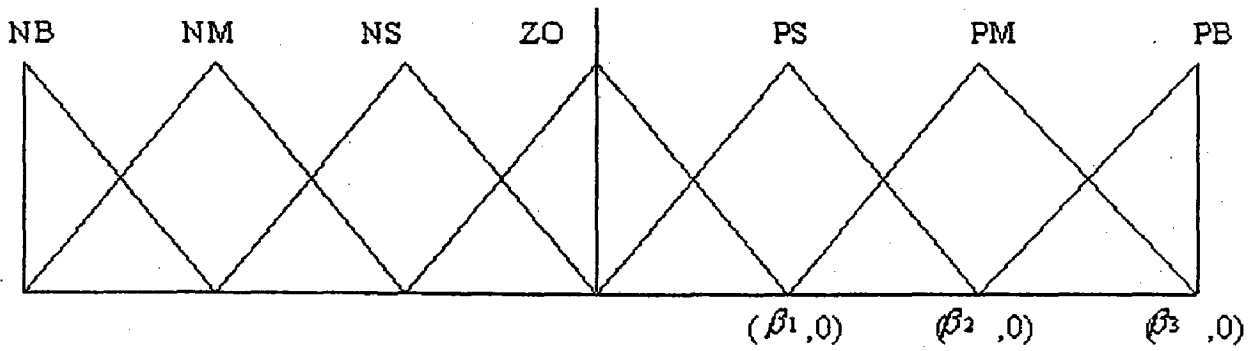


Fig. 2.9(b)

Fig. (2.9) Variation of speed deviation with time.

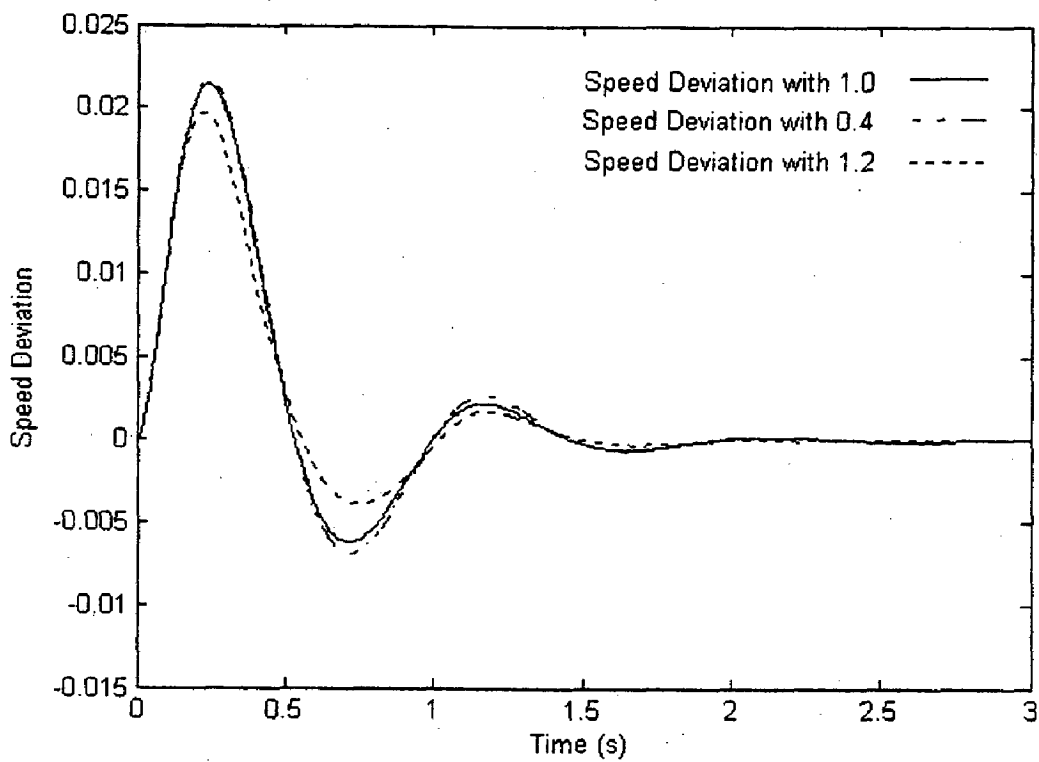


Fig. 2.10 Variation of speed deviation with time

At this stage, we assume that the separation between the peaks vary in geometric ratio i.e.

$\frac{y}{c_1} = \frac{z}{y}$.It can be clearly seen from Fig 3.9(b) that the coordinates of PS, PM and PB are

$(0, \beta_1, \beta_2), (\beta_1, \beta_2, \beta_3)$ and $(\beta_2, \beta_3, \dots)$. $\beta_3 = 3.0$, the positive limit of the universe of

discourse (universe of discourse is -3.0 to 3.0).

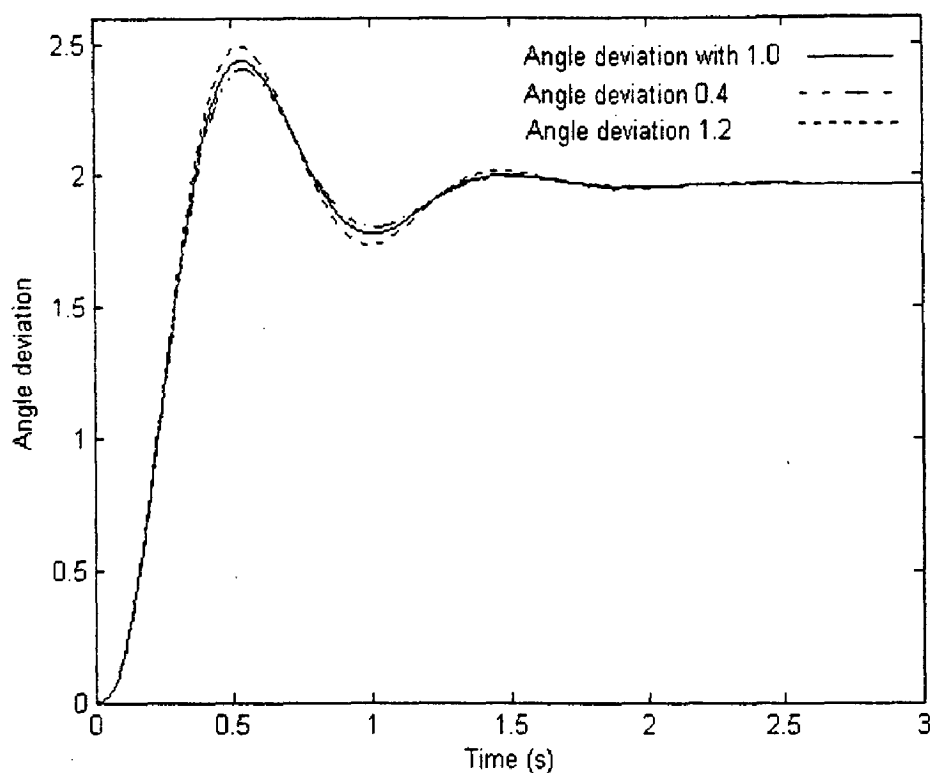


Fig. 2.11 Variation of rotor angle deviation with time

C_1	J	Setting Time		Peak Overshoot	
		$\Delta\omega$	$\Delta\delta$	$\Delta\omega$	$\Delta\delta$
1.2	2.35×10^{-7}	3.4	3.4	0.023	2.6
1.0	2.223×10^{-7}	3.0	3.0	0.020	2.7
0.4	2.217×10^{-7}	2.5	2.5	0.026	2.9

Table 2.2

The value of c_1 is varied over a wide range in order to obtain its optimum value. Figs. 2.10 and 2.11 show the transient response for $\Delta\omega$ and $\Delta\delta$ for a step increase in mechanical torque i.e. $\Delta T_m = 0.05$ pu for $c_1 = 1.2, 1.0$ and 0.4 . Examination of the responses shows that the maximum peak overshoot is nearly the same for $c_1 = 1.2$ and $c_1 = 1.0$ and increases slightly for $c_1 = 0.4$ whereas there is considerable reduction in setting time as c_1 is reduced to 0.4 whereas there is considerable reduction in setting time for c_1

is equal to 0.4. Examination of Table 3.2 shows that the performance index J decreases slightly while the settling time decreases to about 50% with change in c_1 from 1.2 to 0.4. The change in peak deviation is quite insignificant.

CHAPTER-3

Delta –Omega Power System Stabilizer

3.1 Introduction

A lot of research work has been done in the past to find the ways and means to improve dynamic stability of a power system. Present trends in planning and operating of power system are to built power system with less redundancy and operate them closer to transient stability limit. So more reliance and emphasis is being placed on power system controls to provide required compensating effects to reduction in stability margins inherent from present day trends in system design. High gain excitation system equipped with power system stabilizer have been extensively used in modern power system as an effective means of enhancing overall power system stability.

With electric power systems, the change in electric torque of synchronous machine following a perturbation can be resolved in two components, i.e.

$$\Delta T_e = T_s \Delta \delta + T_d \Delta \omega$$

The component of torque change in phase with the rotor angle perturbation $\Delta \delta$ is referred as the synchronizing torque component and the component of torque in phase with the speed deviation $\Delta \omega$ is referred as the damping torque component. system stability depends on the existence of both components of torque for each of the synchronous machine.

The AVR gain plays a major role in system stability. The K_1 - K_6 parameters vary with system loading. Hence magnitude and nature of synchronizing torque component and damping torque component depends on both system loading and AVR gain. Tuning of supplementary excitation controls for stabilizing system modes of oscillations has been subject of much research. The basic tuning techniques utilized with PSS applications are phase compensation and root locus. To provide desired damping, stabilizer transfer function must compensate for the gain and phase characteristics of the excitation system, the generator and the power system, which collectively determine the stabilizer transfer function $GEP(s)$. It is also necessary to recognize the nonlinear nature of power system.

Hence it is a challenge to tune PSS to improve overall system stability over the wide operating range.

In the view of the above, the main objectives of the work presented in this chapter are:

To develop a small perturbation model of a SMIB (single machine infinite bus) system in state space form.

1. To study the effect of system loading on K_1 - K_6 constants.
2. To study the effect of variation AVR gain on stability of system.
3. To develop a small perturbation model of a SMIB (single machine infinite bus) system with delta – omega Power System Stabilizer in state space form.
4. To present a systematic approach for optimizing the parameters of Delta-Omega Power System Stabilizer.
5. To study the effect of variation of system loading condition and system parameters on system dynamic response.

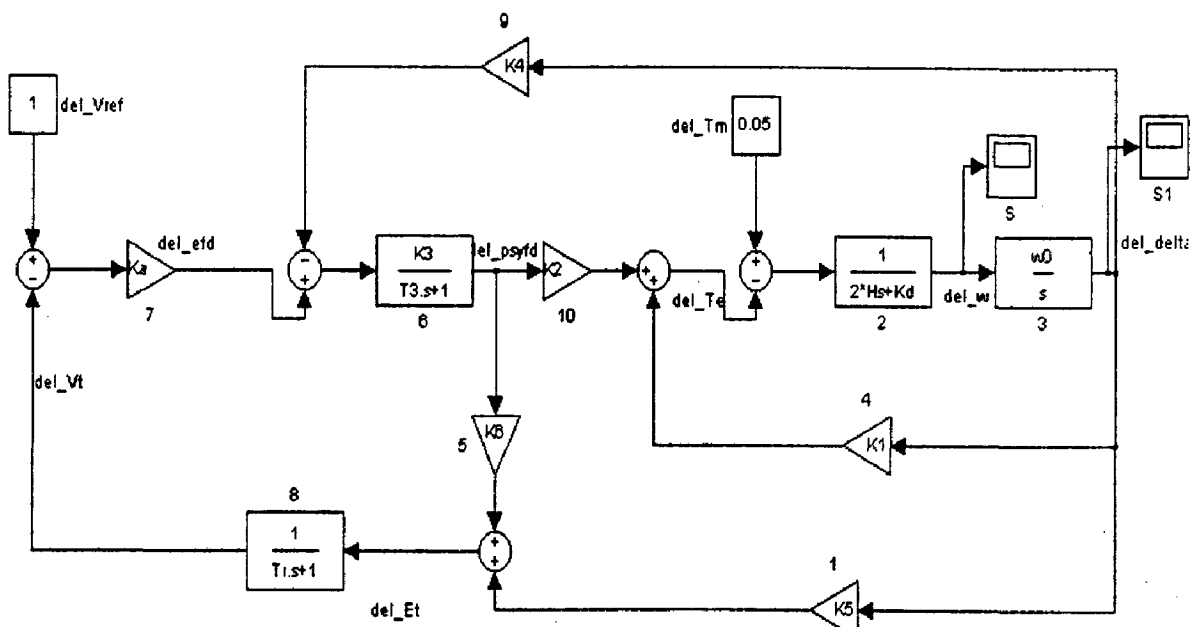


Fig. 3.1 Block Diagram representation of SMIB system with AVR

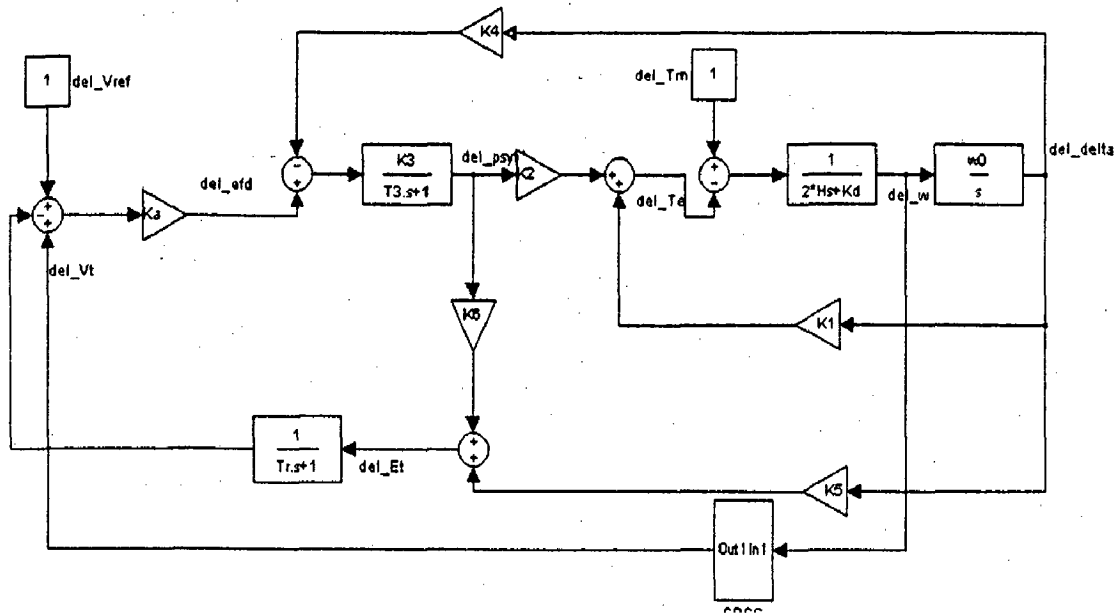


Fig. 3.2 Block Diagram representation of SMIB system Delta-Omega PSS

3.2 System Investigated

Synchronous generator connected to an infinite bus through a transmission line is considered. Thyristor based exciter modern AVR and Delta-Omega PSS have been considered.

3.3 Small perturbation Transfer Function model of SMIB system

As power system is a highly nonlinear system, it is represented by nonlinear differential equations. In stability studies of single machine infinite bus system, researchers have extensively used K_1 - K_6 model, as suggested by Heffron and Philips. The equations to calculate parameters K_1 - K_6 have been derived by liberalizing the system nonlinear equations around an operating point. The same small perturbation model is used in this thesis and is shown in Figure 3.1

3.4 Dynamic model in state space form model of a SMIB system with AVR

The dynamic model in the state space form can be obtained in the form

$$\dot{X} = AX + \Gamma P$$

Where, state vector X is given by

$$X = [\Delta\omega \Delta\delta \Delta\Psi_{fd} \Delta E_{fd}]^{-T}$$

And perturbation vector p is given by

$$p = (\Delta T_m \Delta V_{ref})^T$$

The elements of state matrix A and perturbation matrix Γ are given in Appendix 3.1

3.5 To study the effect of system loading on K1-K6 parameters

The system parameters considered are given in Appendix 3.2 and equations to calculate parameters K₁-K₆ are given in Appendix 3.4. These equations have been derived using small perturbation model, by linearizing the system nonlinear equations around operating point. The active load is varied from 0.1 to 1.0 p.u. and reactive load is varied from -0.3 p.u. to 0.7 p.u. . The variation of parameters with variation in system load is plotted in Figs 3.3. It is observed that all parameters except K₅ are positive and parameter K₅ becomes negative under heavy loading conditions definitions of K₁-K₆ parameters is given in Appendix 3.3.

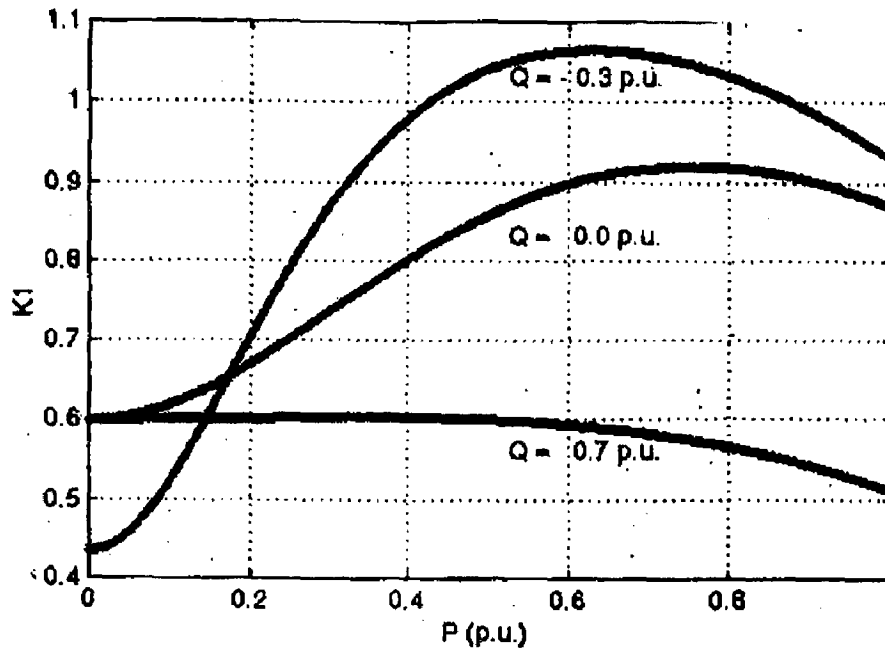


Fig. (3.3 a) Variation of Parameters K₁ with System Loading.

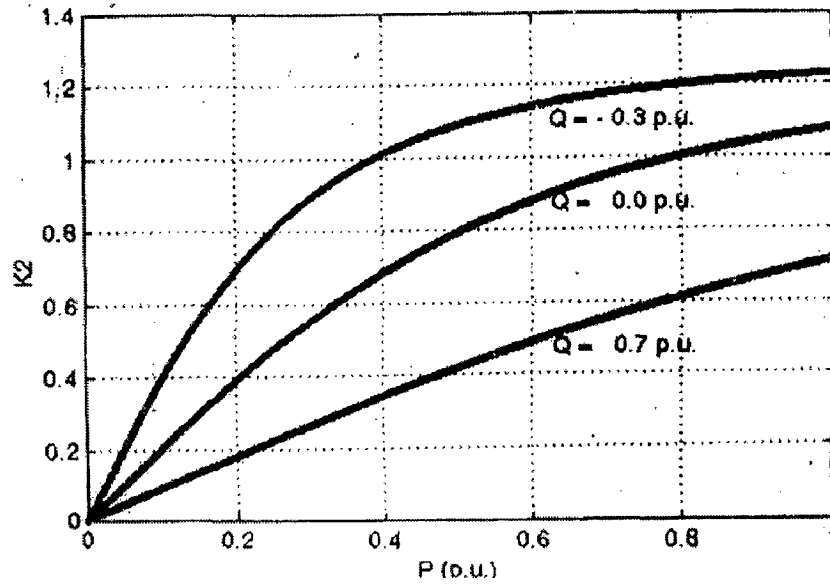


Fig. (3.3 b) Variation of Parameter K_2 with System Loading

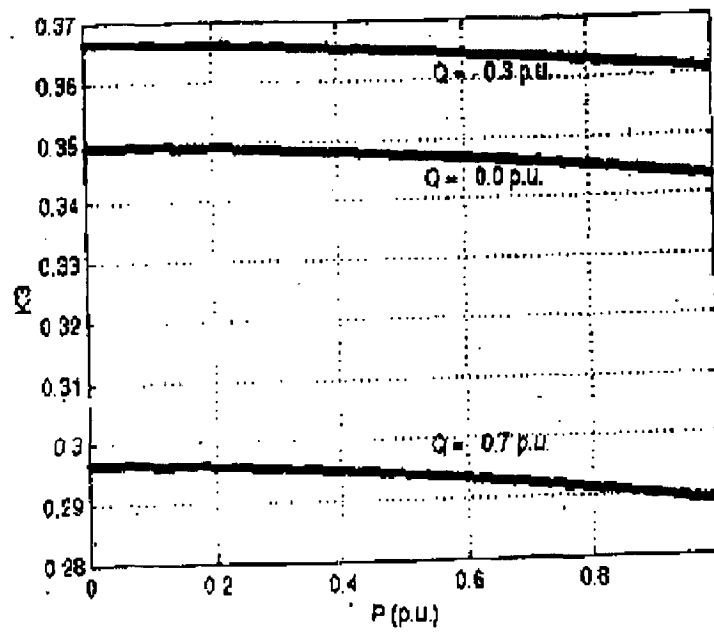


Fig. (3.3 c) Variation of Parameter K_3 with System Loading

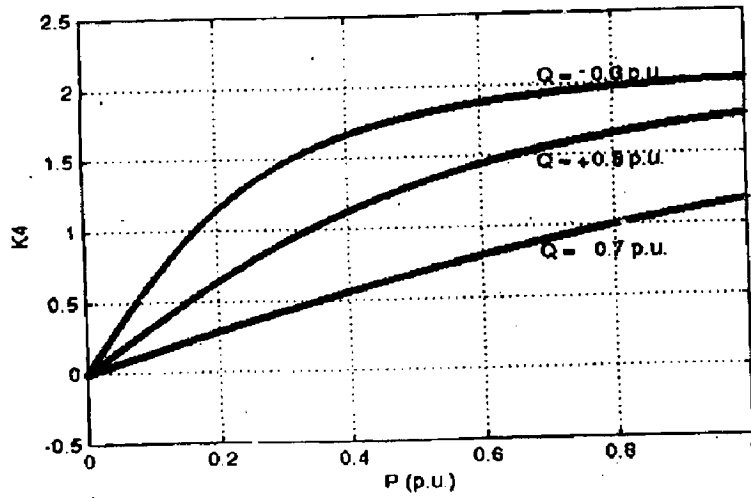


Fig. (3.3 d) Variation of Parameter K_4 with System Loading

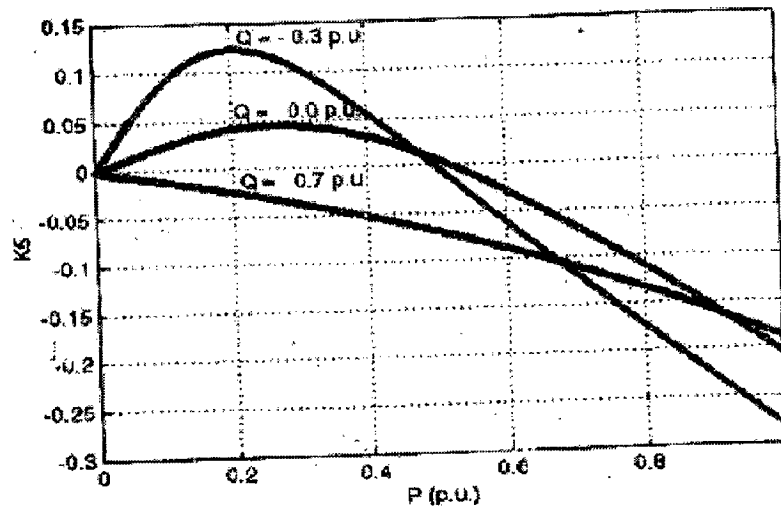


Fig. (3.3 e) Variation of Parameter K_5 with System Loading

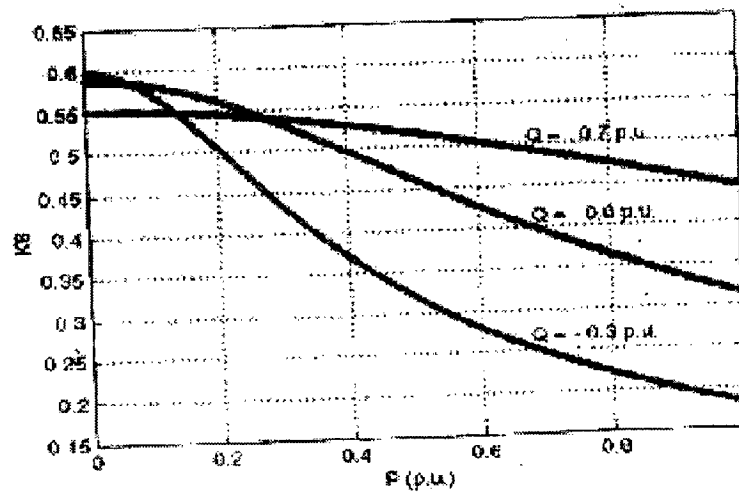


Fig. (3.3 f) Variation of Parameter K_6 with System Loading

3.6 Effect of AVR gain

The effect of variation of AVR gain is studied by computing on synchronizing and damping torque components for loading conditions such that

(a) K_5 is positive

(b) K_5 is negative

From Figures 3.5 it is observed that when K_5 is negative, with the increase in the value of AVR gain from zero damping torque decreases, reaches lowest for $K_a=7$ and the increase with further increase in value of K_a (still remain negative) and becomes zero when K_a reaches infinity. While synchronizing torque first decreases slightly with increase in the value of AVR gain, reaches minimum for $K_a=14$ and then increases with further increase in value of AVR gain K_a .

Under light loading condition, when K_5 is positive, as the value of k_a is increased, the value of synchronizing torque decreases slightly (minimum for $K_a=200$, remains positive) while damping torque increase up to $K_a=55$ and for further increase in K_a , its value decreases but remains positive. Analysis shows that under heavy loading conditions, increase in the value of AVR gain has an adverse effect on system stability.

3.7 Dynamic Model In State Space form of A SMIB system with PSS

The dynamic model in the state space form can be obtained in the form

$$\dot{X} = AX + \Gamma P$$

Where state vector X is given by

$$X = [\Delta\omega \Delta\delta \Delta\Psi_{fd} \Delta E_{fd} \Delta V_1 \Delta V_2 \Delta V_3]^T$$

and perturbation vector p is given by

$$P = \begin{pmatrix} \Delta T_m \\ \Delta V_{ref} \end{pmatrix}$$

The elements of state matrix A and perturbation matrix Γ are given in Appendix 3.5.

instability point. In practice the final PSS gain should be at least a factor of 2-3 (6-10dB) less than the instability gain. With the integral of accelerating power design the gain margins are typically much in excess of 10dB at times approaching 20dB.

- (2) The change in local mode frequency with and without PSS in operation should be less than 10%. In other words the PSS gain should be selected to limit the effect of the stabilizer on the synchronizing torque coefficient.

3.9 Dynamic performance of the system

The PSS is designed to give desired damping over the operating range. Dynamic response of the system for 0.05 p.u. Increases in mechanical torque over the wide operating range have plotted (Figures 3.5 to 3.6e).

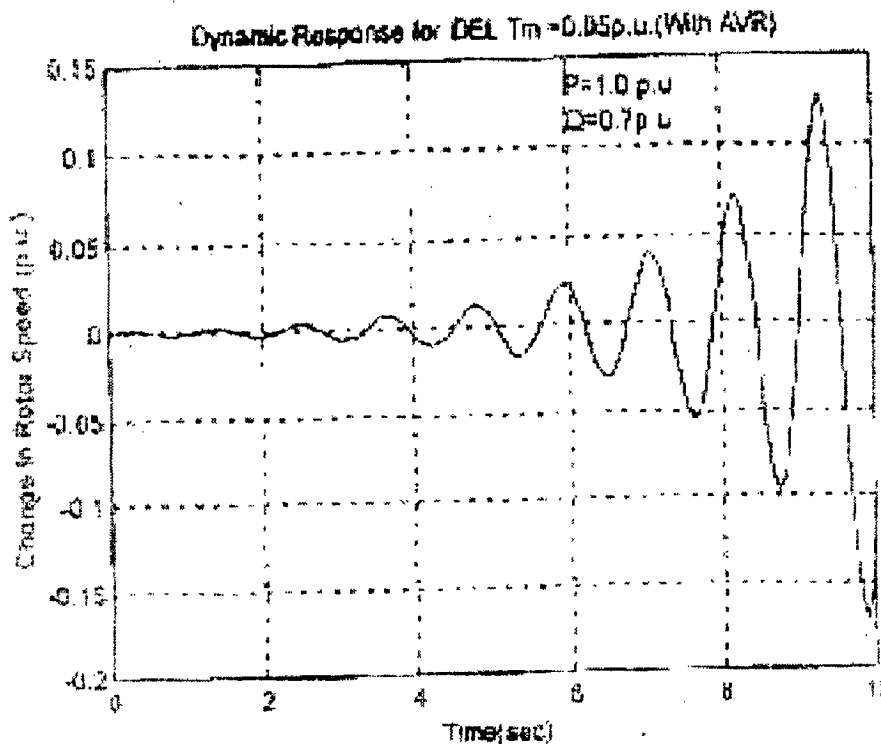


Fig. 3.5 (a) Dynamic response without PSS
Rotor Speed variation for $\Delta T_m = 0.05$ p.u.

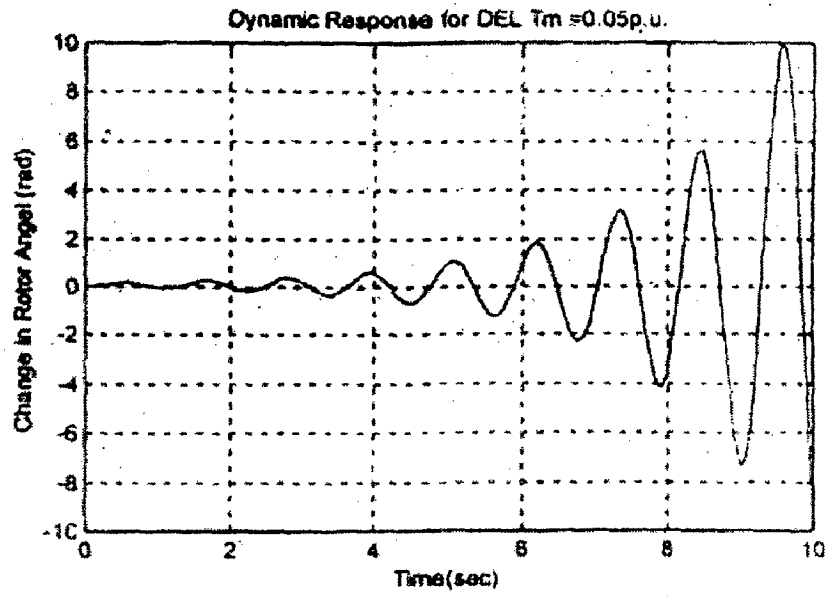


Fig. 3.5 (b) Dynamic response without PSS
Rotor angle variation for $\Delta T_m = 0.05$ p.u.

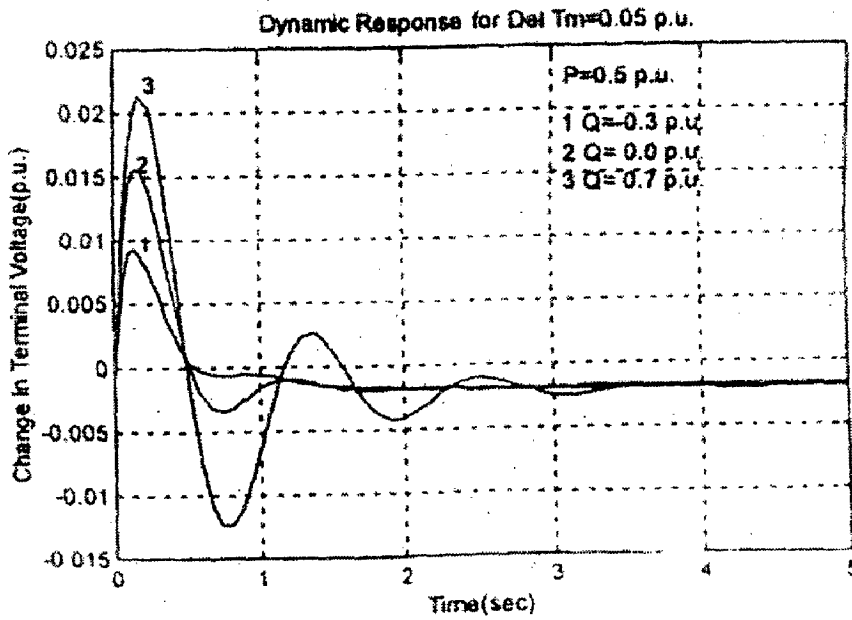


Fig. 3.6(a) Dynamic response with PSS
Rotor speed variation for $\Delta T_m = 0.05$ p.u.

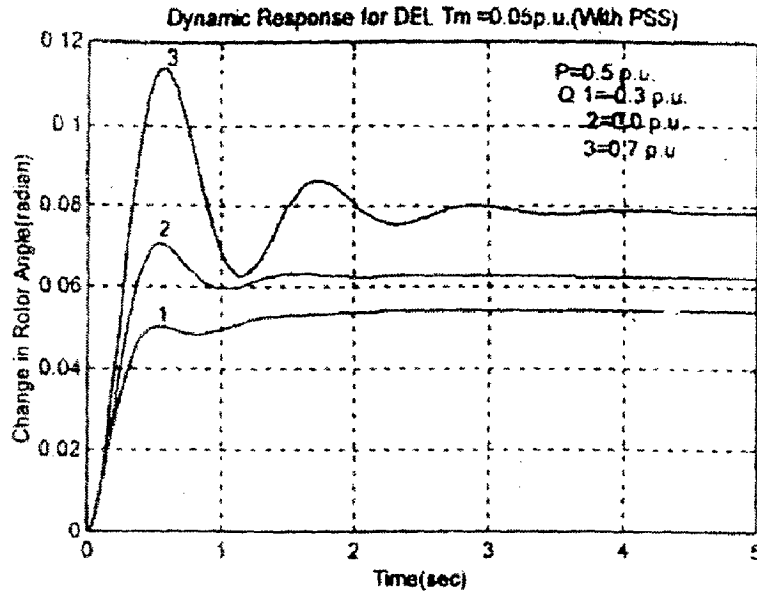


Fig. 3.6 (b) Dynamic response with PSS
Rotor angle variation for $\Delta T_m = 0.05$ p.u.

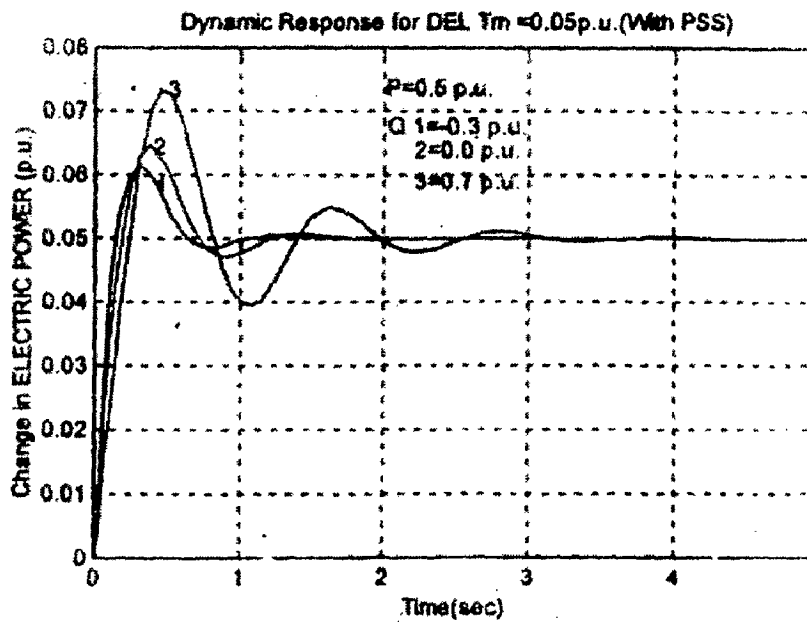


Fig. 3.6 (c) Dynamic response with PSS
Terminal Power variation for $\Delta T_m = 0.05$ p.u.

3.6 Effect of AVR gain

The effect of variation of AVR gain is studied by computing on synchronizing and damping torque components for loading conditions such that

- (a) K_5 is positive
- (b) K_5 is negative

From Figures 3.5 it is observed that when K_5 is negative, with the increase in the value of AVR gain from zero damping torque decreases, reaches lowest for $K_a=7$ and the increase with further increase in value of K_a (still remain negative) and becomes zero when K_a reaches infinity. While synchronizing torque first decreases slightly with increase in the value of AVR gain, reaches minimum for $K_a=14$ and then increases with further increase in value of AVR gain K_a .

Under light loading condition, when K_5 is positive, as the value of k_a is increased, the value of synchronizing torque decreases slightly (minimum for $K_a=200$, remains positive) while damping torque increase up to $K_a=55$ and for further increase in K_a , its value decreases but remains positive. Analysis shows that under heavy loading conditions, increase in the value of AVR gain has an adverse effect on system stability.

3.7 Dynamic Model In State Space form of A SMIB system with PSS

The dynamic model in the state space form can be obtained in the form

$$\dot{X} = AX + \Gamma P$$

Where state vector X is given by

$$X = [\Delta\omega \Delta\delta \Delta\Psi_{fd} \Delta E_{fd} \Delta V_1 \Delta V_2 \Delta V_3]^{-T}$$

and perturbation vector p is given by

$$p = \begin{pmatrix} \Delta T_m \\ \Delta V_{ref} \end{pmatrix}$$

The elements of state matrix A and perturbation matrix Γ are given in Appendix 3.5.

3.8 Design of Robust Delta-Omega Power System Stabilizer

Due to nonlinear nature of power system, if the PSS is designed for optimal performance about an operating point, its performance would be sub optimal at other operating points. Hence PSS is designed to give desired performance over the wide operating range. the operating range considered for design is

- (a) Active load variation from 0.5 p.u. to 1.0 p.u.
- (b) Reactive load variation from -0.3 p.u. to 0.7 p.u.
- (c) Frequency of rotor oscillation from 0.2 Hz to 2.5 Hz.

The delta-omega Power System Stabilizer has three parts:

- (1) Phase compensation block
- (2) Washout block
- (3) Stabilizer Gain

The transfer function block diagram representation of system PSS is shown in Figure 3.2 and Delta-Omega PSS is shown in Figure 3.4.

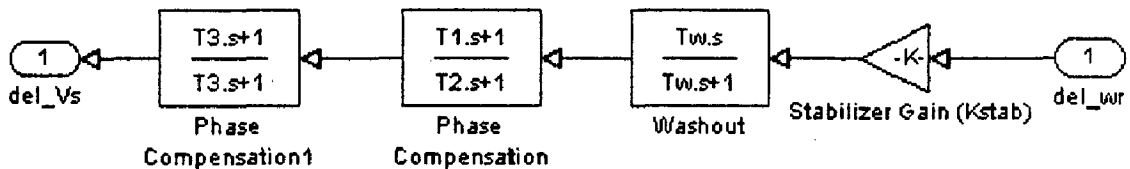


Fig.3.4 Delta-Omega Power System Stabilizer

3.8.1 Phase Compensation Block

As mentioned earlier, to provide damping stabilizer transfer function must compensate for the gain and phase characteristics of the excitation system, the generator and the power system. $GEP(s)$ is the transfer function from the stabilizer output to the component of electric torque. if the exciter transfer function $G_{ex}(s)$ and the generator transfer function between ΔE_{fa} and ΔT_e were pure gains, a direct feedback of $\Delta \omega_r$ would result in pure damping component. However in practice they exhibit a frequency dependent gains and phase characteristic. Therefore the PSS transfer function should

have appropriate phase compensation circuits to compensate for phase between exciter input and electric torque. In the ideal case, with the phase characteristic of GPSS (s) being an exact inverse of the exciter and generator phase characteristics to be compensated, the PSS would result in pure damping torque at all oscillating frequencies. If the phase lead network provides more compensation than the phase lag between ΔT_e and ΔV_s , the PSS introduces a negative synchronizing torque component and vice versa. Usually the PSS is required to contribute to the damping of rotor oscillations over a range of frequencies (0.2Hz to 2.5 Hz), so phase lead network should provide compensation over this frequency range. So a compromise is made and a characteristic acceptable for different system conditions is selected. Generally under compensation upto-45 degree is acceptable as reported in literature [5].

3.8.2 Signal Washout block

The signal washout block serves as high pass filter. With the time constant T_w high enough to allow signals associated with oscillations in ω_r to pass unchanged. Without it steady changes in speed would modify the terminal voltage. From the viewpoint of washout function, the value of T_w is not critical and may be in the range of 1 sec to 20 seconds. The main consideration is that it be long enough to pass stabilizing signals at the frequencies of interest unchanged, but not so long that it leads to undesirable generator voltage excursions during system islanding conditions. As recommended in the literature [5], washout time constant equal to 10 seconds is considered for further investigation in this thesis.

3.8.3 Stabilizer Gain

The stabilizer gain determines the amount of damping introduced by the stabilizer. The damping of electromechanical mode increases with the stabilizer gain, while damping of control mode decreases.

The choice of the best PSS gain requires consideration of a number of factors:

- (1) As the local mode root damping is increased, there is another mode, sometimes called the exciter mode or control mode, which decreases in damping. If the PSS gain is increased to the value where exciter mode becomes unstable is called the

instability point. In practice the final PSS gain should be at least a factor of 2-3 (6-10dB) less than the instability gain. With the integral of accelerating power design the gain margins are typically much in excess of 10dB at times approaching 20dB.

- (2) The change in local mode frequency with and without PSS in operation should be less than 10%. In other words the PSS gain should be selected to limit the effect of the stabilizer on the synchronizing torque coefficient.

3.9 Dynamic performance of the system

The PSS is designed to give desired damping over the operating range. Dynamic response of the system for 0.05 p.u. Increases in mechanical torque over the wide operating range have plotted (Figures 3.5 to 3.6e).

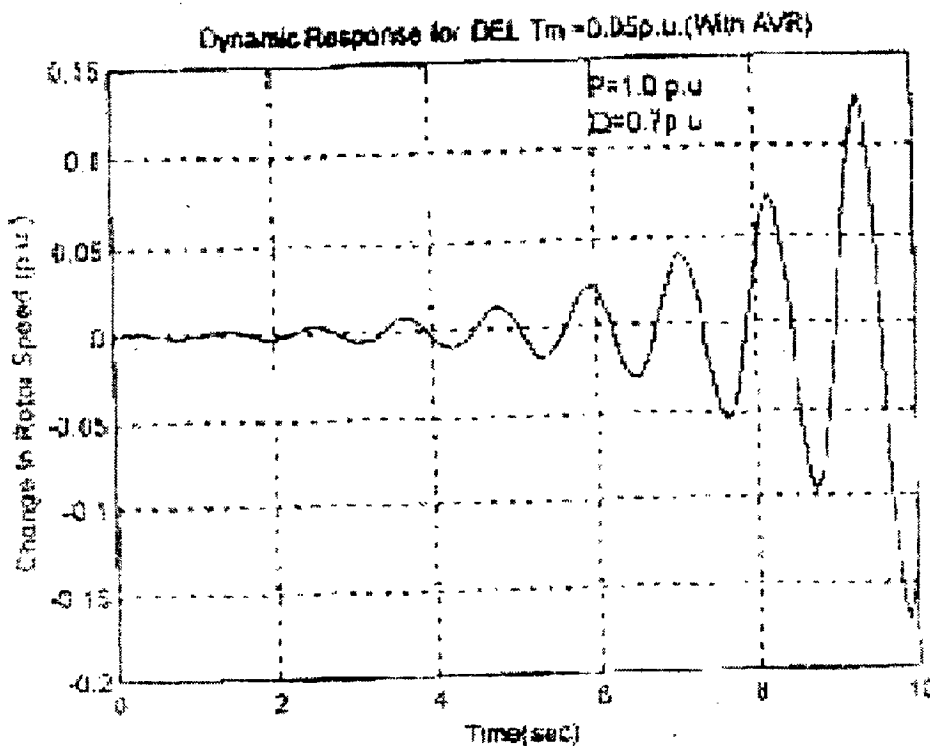


Fig. 3.5 (a) Dynamic response without PSS
Rotor Speed variation for $\Delta T_m = 0.05$ p.u.

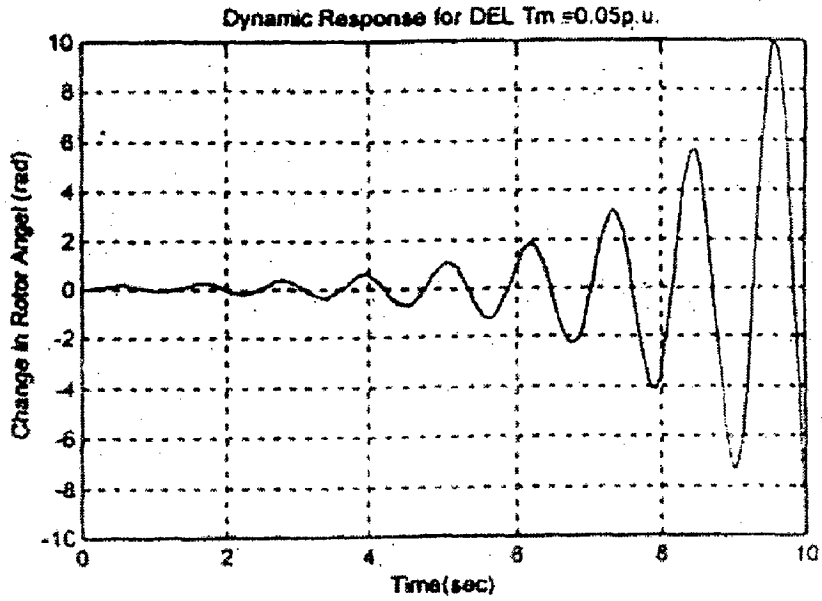


Fig. 3.5 (b) Dynamic response without PSS
Rotor angle variation for $\Delta T_m = 0.05$ p.u.

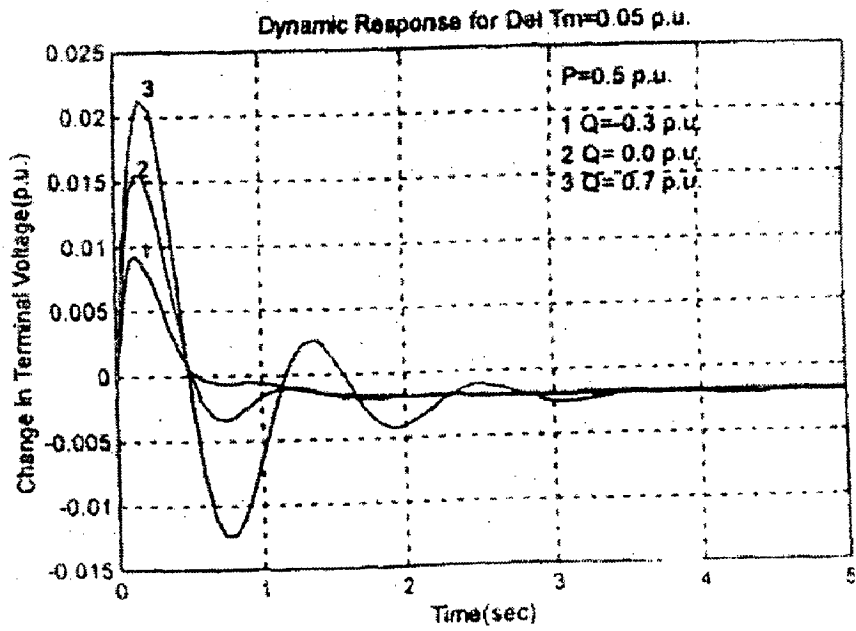


Fig. 3.6(a) Dynamic response with PSS
Rotor speed variation for $\Delta T_m = 0.05$ p.u.

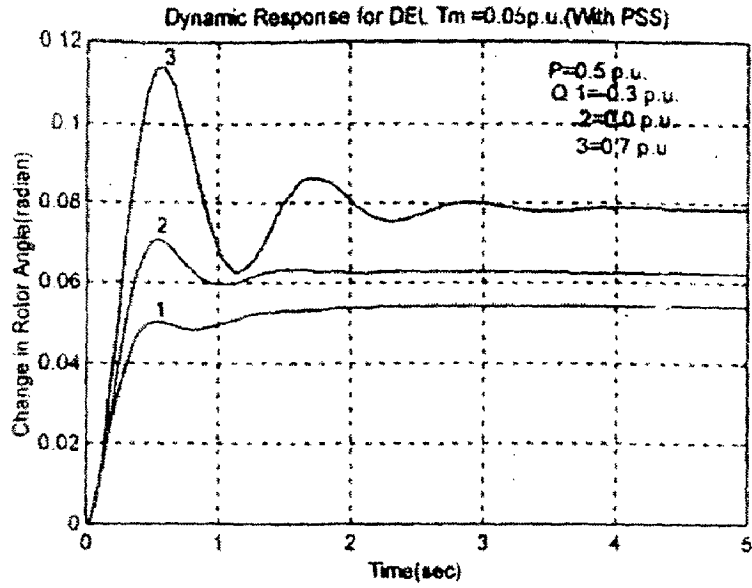


Fig. 3.6 (b) Dynamic response with PSS
Rotor angle variation for $\Delta T_m = 0.05$ p.u.

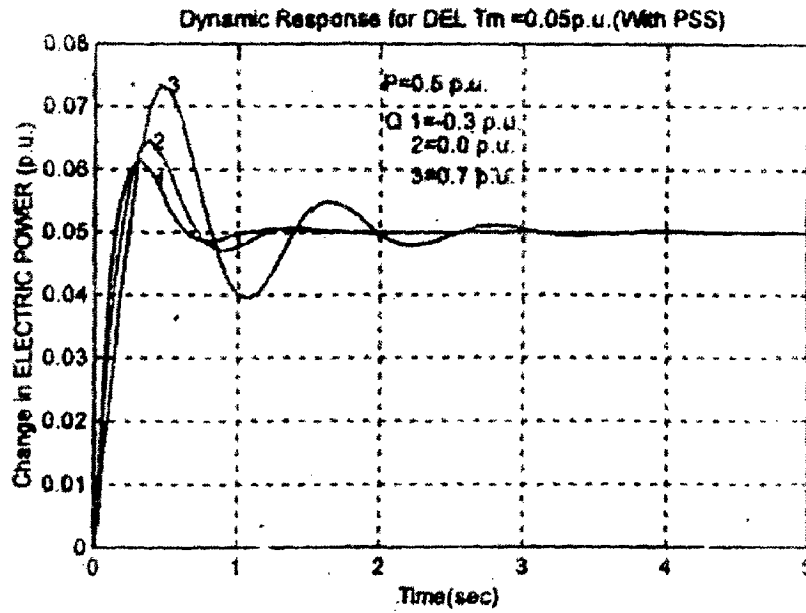


Fig. 3.6 (c) Dynamic response with PSS
Terminal Power variation for $\Delta T_m = 0.05$ p.u.

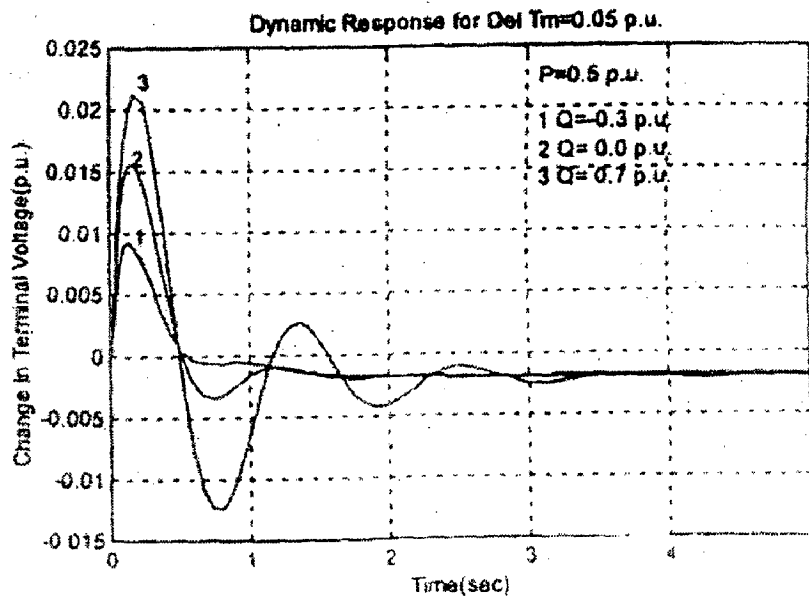


Fig. 3.6 (d) Dynamic response with PSS
Terminal Voltage variation for $\Delta T_m = 0.05$ p.u.

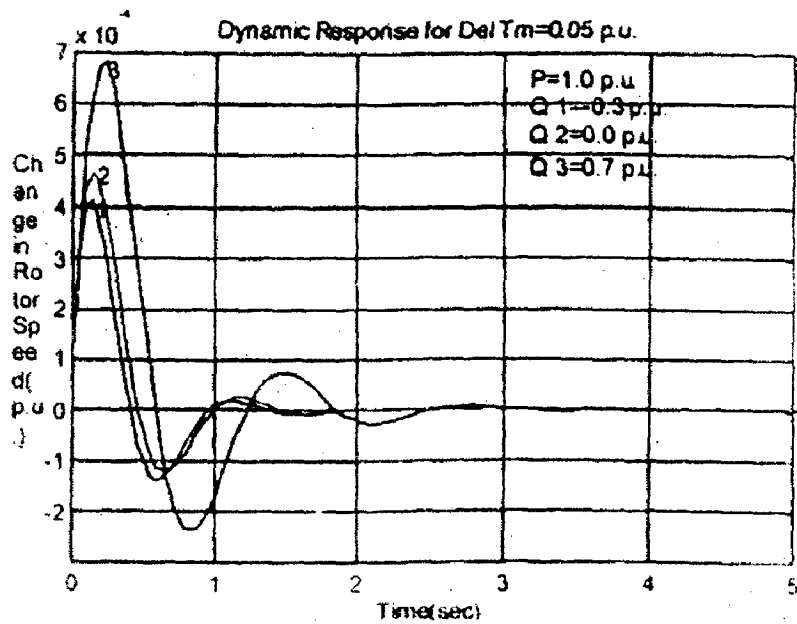


Fig. 3.6 (e) Dynamic response with PSS
Rotor speed variation for $\Delta T_m = 0.05$ p.u.

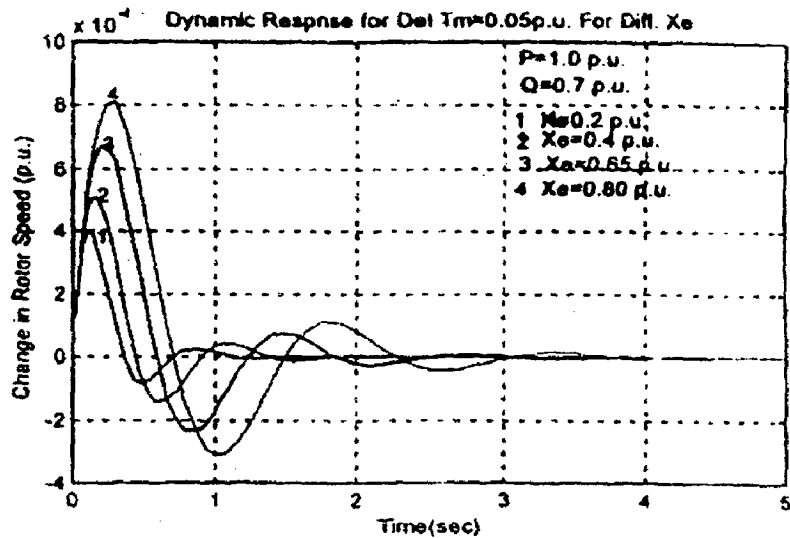


Fig. 3.7 Dynamic response with PSS
 Rotor speed variation for $\Delta T_m = 0.05$ p.u. &
 Different values of External Reactance (0.2 p.u. to 0.9 p.u.)

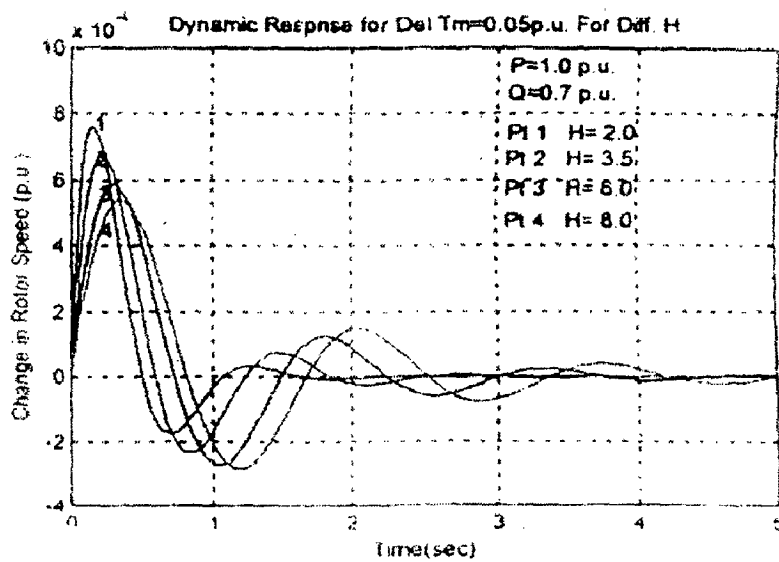


Fig. 3.8 Dynamic response with PSS
 Rotor speed variation for $\Delta T_m = 0.05$ p.u. &
 Different values of Inertia Constant (2 to 8 MJ/MVA)

Sensitivity analysis is also carried out to know the effect of variation of system loading and parameters on system dynamic response. for the operating for P=1.0 p.u. and Q=0.7 p.u. the dynamic response of the system. With and without PSS, following 5% step increase in mechanical torque is plotted (Figures 3.10 qnd 3.11e). It is observed that response settles down satisfactorily with PSS i.e. response settles down to their steady state value in about less than 3 seconds. As it is clear from Figure 3.10, system is unstable without PSS.

The eigen value analysis for the same operating condition i.e. P=1.0 p.u. and Q=0.7 p.u. is also carried out which reveals that damping ratio for electromechanical mode increases with PSS from -0.11 to +0.4245. the eigen value analysis is presented in

Eigen Value Without PSS					Eigen Value With PSS				
Real	ω_d	Damping-Ratio	ω_n	Mode	Real	ω_d	Damping-Ratio	ω_n	Mode
-51.86					-53.53				
+0.609	+5.45	-0.111	5.48	Electro-mech	-13.08		0.756	17.287	Excitor Mode
	-5.45	-0.111	5.48	Electro-mech	-13.08		0.756	17.287	Excitor Mode
-12.89					-45.89				
					-2.33	+4.97	0.424	5.487	Electro mech
					-2.33	-4.97	0.424	5.487	Electro mech
					-0.10				
					-6.89				

Table-3

3.10 Sensitivity analysis

The operating conditions and system parameters never remains constant and PSS parameters once tuned cannot changes on system dynamic performance.

3.10.1 Effect of variation in real power P

Figures 3.6(a) and 3.6(e) shows the responses for $\Delta\omega$ for a small step perturbation in T_m ($=0.05$ p.u.), with real power varying from 0.5 p.u. to 1.0p.u. peak deviation in rotor speed $\Delta\omega$ slightly and settling time also decreases. It may thus inferred that dynamic responses are quite insensitive to wide variation in p.

3.10.2 effect of change in reactive power Q

Figures 3.6 a to 3.6 e show the responses for $\Delta\omega, \Delta\delta, \Delta E_t$ and ΔP_e for small step perturbation in T_m ($=0.03$ p.u.), with reactive power Q varying from -0.3 p.u. to 0.7 p.u., peak deviation in all rotor speed deviation $\Delta\omega$, terminal voltage deviation ΔE_t , terminal power deviation ΔP_e and settling time, all increases slightly. However system remains stable. It may thus be inferred that dynamic responses are quite insensitive to wide variation in Q.

3.10.3 Effect of change in transmission line reactance X_e

Figure 3.7 shows the response for $\Delta\omega$ for small step perturbation in T_m ($=0.05$ p.u.), with transmission line reactance X_e varying from 0.2 p.u. to 0.9 p.u., both, peak deviation in rotor speed $\Delta\omega$ and settling time, both increases slightly. However system remains stable. It may thus be inferred that dynamic responses are quite insensitive to wide variation in transmission line reactance X_e .

3.10.4 Effect of change in inertia constant H

Figure 3.8 shows the responses for $\Delta\omega$ for small step perturbation in T_m ($=0.05$ p.u.), with inertia constant H varying from 2.0MJ/MVA to 8.0 MJ/MVA, peak deviation in rotor speed $\Delta\omega$ decreases slightly while settling time increases slightly. It may thus be

inferred that dynamic responses are quite insensitive to wide variation in inertia constant H .

3. 11 Conclusion

The following are the significant conclusions of work presented in this chapter

- (1) Small perturbation model of SMIB system in state space form, with and without PSS has been developed.
- (2) Studies show that parameter K_5 plays very important role in determining the small signal stability of the system. If K_5 is negative, increase in value of AVR gain adversely affects the small signal stability.
- (3) A systematic approach has been introduced to tune the Delta-Omega PSS using frequency domain techniques.
- (4) A detailed sensitivity analysis shows that the system dynamic responses are quite insensitive to wide variations in system loading conditions and parameter variations.

4.1 Introduction

The enhancement of damping of electromechanically oscillations in a multi machine power system by the application of power system stabilizers has been the subject of great attention and is much more important today when many large and complex power systems frequently operate close to their stability limits. Most of the work on application of power system stabilizers is connected with the tuning of their parameters to achieve satisfactory damping characteristics of an inter connected system.

The identification of optimum stabilizer locations is very important in a multi machine system. The stabilizers installed and tuned at arbitrary locations in a network may not be very effective. One of the most commonly used approach stabilizer sitting is the eigenvector method proposed by De Mello [8]. In this method the eigenvector corresponding to each eigen value is obtained. By observing the eigenvector, it is possible to identify the generator location, which affects a particular swing mode the most. One of the problems in using the right eigenvector for identifying the relationship between the states and swing modes is that the elements of the eigen vectors are dependent on units and scaling associated with the state variables. Although this method has been successfully applied to some power systems, it may fail in certain systems with generators of rather different rated capacities. In fact it has been found in recent study that the eigenvector itself may lead to undesirable stabilizer locations.

Another method, the frequency domain method, based on concept of coherent groups [13] was proposed for improving the total system. Although this method was successfully tested [15]; it suffers from arbitrations concerning the selection of a particular site for power system stabilizer application within one coherent group, which cannot be overcome without extensive investigations of dynamic performances of stabilized systems under various combinations of selected generators.

Recently, the concept of participation factors was shown to be valuable and feasible means for resolving this problem [18], but it is still restricted to the sequential power

system stabilizer application, which considers the enhancement of damping of just one critical electromechanical mode at a time.

In this chapter an approach for exact identification of machines where the application of stabilizers ensure maximum improvement of overall system damping characteristics using Sensitivity and Participation methods are presented.

4.2. Methods of PSS location

The PSS location selection problem has been studied for a long time. There are various methods for the selection of the PSS location. Some of these methods are:

1. Right-eigen vector method.
2. Participation factors
3. Sensitivity of PSS effect (SPE).
4. Optimal Location of Power System Stabilizers Based on Probabilistic Analysis.

1. Right-eigen vector method

The right – eigen vector method [16], which uses the right-eigenvector information of a mode to identify the best PSS location. This approach is based on the consideration that the right-eigenvector entries measure the activity of the state variables participating in an oscillation mode and these state variables may be used as PSS input.

According to this method PSS should be locate on that which has maximum value of $|\mu_{\Delta\omega}|$. Where $|\mu_{\Delta\omega}|$ is the amplitude of the right-eigenvector entry corresponding to machine speed ($\Delta\omega$).

2. Participation factors

One problem is using right and left eigenvectors [18] individually for identifying the relationship between the states and the modes is that the elements of the eigenvectors are dependent on units and scaling associated with the state variables. As a solution to this problem, a matrix called the participation matrix (P), which combines the right and left eigenvectors as a measure of the association between the state variables and the modes.

$$P = [P_1 P_2 \dots P_3]$$

$$\text{With } p_{ki} = \Phi_{ki} \Psi_{ik}$$

$$p_{ki} = \Phi_{ki} \Psi_{ik}$$

Where

Φ_{ki} = The element on the kth row and ith column of the modal matrix Φ
 = kth entry of the right eigenvector Φ_i

Ψ_{ki} = The element on the ith row and kth column of the modal matrix Ψ .
 = kth entry of the left eigenvector Ψ_i .

The element $p_{ki} = \Phi_{ki} \Psi_{ik}$ is termed the participation factor. It is a measure of the relative participation of the kth state variable in the ith mode, and vice-versa.

The machine, which has highest participation factor, is best for the PSS location.

3.Sensitivity of PSS Effect

If a machine is selected for PSS installation, for best affect the amplitude of PSS input (measured by right-eigenvector) should be relatively large, and second the control effect of PSS should also be strong.

In the right-eigenvector information to identify the best PSS locations. Therefore the result of this method may be misleading. In the participation method also does not control effect of PSS.

In order to take into consideration both PSS input and PSS control effect in selecting PSS location[16], sensitivity of PSS Effect (SPE) for a machine (jth) is defined as follows:

$$SPE_j = \mu_{\Delta\omega_j} \nu_{\Delta E_{fdj}} \frac{k_{ej}}{t_{ej}} \quad (j = 1, \dots, m)$$

Where, $\mu_{\Delta\omega_j}$: right eigenvector entry corresponding to $(\Delta\omega_j)$,

Supposing speed is used as PSS inpu.

$\nu_{\Delta E_{fdj}}$: Left eigenvector entry corresponding to state ΔE_{fdj}

SPE measure both the activity of PSS input $(\Delta\omega_j)$ participating in a certain mode of oscillation and the control effect of PSS on this mode. The larger the amplitude of SPE the better the overall performance of PSS, if installed.

1.4. Optimal Location of Power System Stabilizers Based on Probabilistic Analysis

The probabilistic approach for the optimum location of power system stabilizers (PSSs). When the variation of nodal injected power representing various load levels is described by statically attributes and considered in eigenvalue analysis, the probabilistic distribution of a eigen value will be expressed by its expectation and variance under the assumption of normal distribution. The utilization of PSSs will improve both of the expectations and variances for the critical eigenvalue. This method therefore calculated, not only the sensitivity coefficients, which are, accomplished distributions of these sensitivity coefficients which are accomplished by means of the second order sensitivity calculation of eigenvalues with respect to nodal injections and PSS gains.

1.5 Coupling Factors

The coupling factors give the mutual coupling between two generators affected a particular mode. The coupling between the i th and j th machine in a particular oscillatory mode h is defined as

$$C_{ij}(h) = \frac{P_{ih} P_{jh}}{M_i M_j} \quad (3.12)$$

Where

P_{ih} = participation factor of i th machine in h th mode.

P_{jh} = participation factor of j th machine in h th mode.

M_i = moment of inertia of i th machine,.

M_j = moment of inertia of j th machine.

The total coupling factor, which weights the influence of stabilizers applied over machines I and j on their dynamic behavior under simultaneous excitation of all

$$C_{ij} = \sum_h C_{ij}(h) \quad (3.13)$$

The coupling factor defined in equation (3.13) represents a suitable and reliable base for identification of the most effective combination of generators for system stabilizer application, yielding maximum enhancement of the total system stability.

4.3 Optimum PSS Site

In our example we will use the Participation factor and Sensitivity method for PSS location. According to Participation method which machine has the highest value of participation factor will be best suited for PSS location.

According to Sensitivity method PSS will be located at that machine which has the highest value of Sensitivity factor.

4.4 Optimum Location of PSS for Multi-Machine System

A 3-machine 9-bus system [3] is used for determine the optimal location of the PSS. The linear model of the system is shown in the Fig 1. and data of the system are shown in the table1 and eigen values are shown in table2.

First Participation factor method and Sensitivity Method are used for PSS location.

The following table is given below which show the damping ratio and participation factor of the corresponding swing modes.

A 3-machines, 9-buses system is used in this work. The oscillation behavior of the system is calculated with the help of eigen analysis.

A 3-machines, 9-buses system is shown in the fig and data are given in the tables.

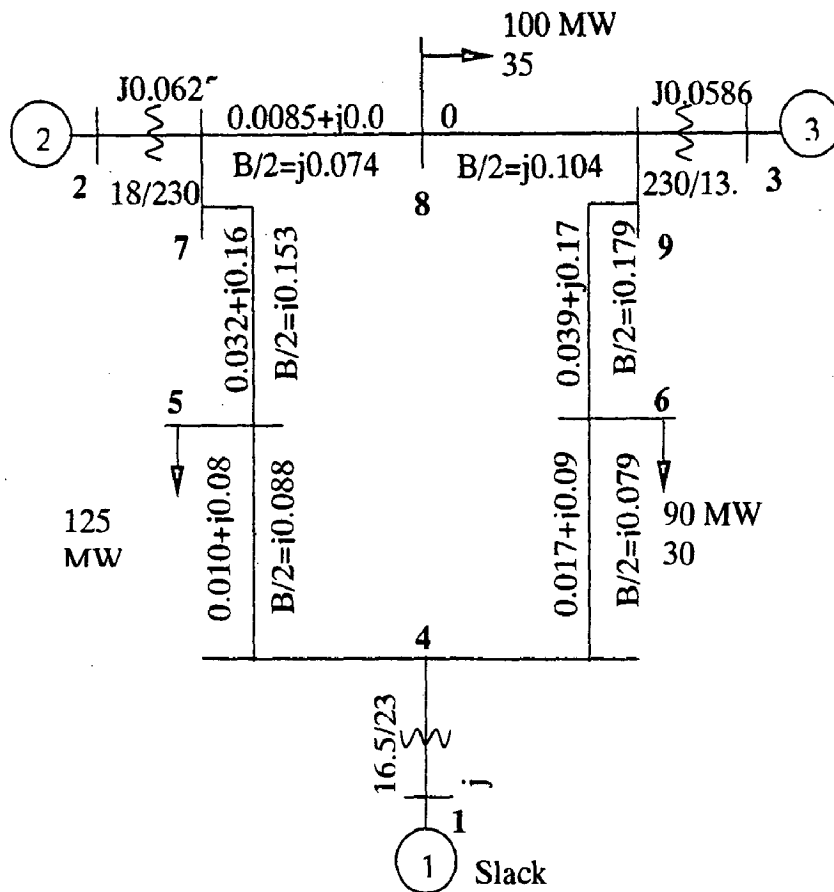


Fig. 4.1:WSCC 3-machine, 9-bus system
all impedances are in pu on a 100-MVA base

(Generator Data)

Generator No.	1	2	3
Rated MVA	247.5	192.0	128.0
kV	16.5	18.0	13.8
H(sec)	23.64	6.4	3.01
Power Factor	1.0	0.85	0.85
Type	Hydro	Steam	Steam
Speed	180r/min	3600r/min	3600r/min
x_d	0.1460	0.8958	1.3125
x_d'	0.0608	0.1198	0.1813
x_q	0.0969	0.8645	1.2578
x_q'	0.0969	0.1969	0.25

x_1 (leakage)	0.0336	0.0521	0.0742
T_{do}	8.96	6.00	5.89
T'_{q0}	0	0.535	0.600
Stored energy at rated speed	2364MW.s	640MW.s	301MW.s

Then with the help of above data for 3-machines and 9-buses system the eigen values can be calculated which is shown in the following table. From this it is possible to calculate the Right eigen vector, Left Eigenvector and participation factors.

Participation Factor:

Swing Mode	Eigen Value (λ)	Frequency (f) Hz	Damping Ratio (ξ)	Machine No.	Participation Factor
1.	-0.7209+j12.7486	2.02	0.056	3	0.41
2.	-0.1908+j8.3672	1.33	0.022	2	0.32

Sensitivity Method:

Mode No	G1(g1)	G2(g2)	G3(g3)
1.	0.0000	0.7765	14.4264
2.	0.6914	2.7610	1.7593
3.	1.9148	0.7765	1.4074

In participation methods, participation factor is calculated for corresponding to each machine. Like in our case machine 3 has the maximum participation factor, so Machine 3 will be best suited for PSS location.

In sensitivity method, sensitivity is calculated for each machine and which has highest value of sensitivity is best suited for PSS location. In our model machine 3 has the highest value of sensitivity, so machine 3 will be best suited for PSS location.

5.1 Introduction

To provide damping to rotor oscillations, the stabilizer must produce a component of electrical torque in phase with the speed variations. The implementation details may differ, depending upon the stabilizer input signal employed. However, for any input signal the transfer function of the stabilizer must compensate for the gain and phase characteristics of the excitation system, the generator and the power system, which collectively determine the transfer function, from the stabilizer output to the component of electrical torque, which can be modulated via excitation control.

Kundur et al [] have presented a comprehensive study pertaining to power system stabilizer. Two alternative excitation control schemes were considered, one with and one without transient gain reduction. It has been shown that with appropriate selection of stabilizer parameters both schemes provide satisfactory overall performance. The importance of appropriate choice of washout time constant and stabilizer output limits in addition to phase lead compensation parameters has been demonstrated. However no systematic approach for designing power system stabilizer parameters has been presented.

5.2 Illustrative system Example

We have considered the popular Western System Coordinated Council (WSCC) 3-machine, 9-bus system [3] shown in Fig.1. The base MVA is 100, and system frequency is 60 Hz. The system data are given in Appendix I. The system has been simulated with classical model for the generators. The disturbance initiating the transient is a three phase-fault occurring near bus 7 at the end of line 5-7. Opening of line 5-7 clears the fault. The system, while small, is large enough to be nontrivial and thus permits the illustration of a number of stability concepts and results.

5.3 System Modeling

The complete system has been represented in terms of Simulink blocks in a single integral model. It is self-explanatory with the mathematical model given below. One of the most important features of a model in Simulink is its tremendous interactive capacity. It makes the display of a signal at any point readily available, all one has to do is to add a Scope block there or an output port alternatively. Giving a feedback signal is also as easy as drawing a line. A parameter within any block can be controlled from Matlab command line or through an m-file program. This is particularly useful for transient stability study as the power system configurations differ before fault, during fault and after fault. Loading conditions and control measures can also be implemented accordingly

5.3.1 Mathematical Modeling of The system

Once the Y matrix for each network condition (pre-fault, during and after fault) is calculated, we can eliminate all the nodes except for the internal generator nodes and obtain the Y matrix for the reduced network. The reduction can be achieved by matrix operation with the fact in mind that all the nodes have zero injection currents except for the internal generator nodes. In the power system with n generators, the nodal equation can be written as:

$$\begin{bmatrix} I_n \\ 0 \end{bmatrix} = \begin{bmatrix} Y_{nn} & Y_{nr} \\ Y_{rn} & Y_{rr} \end{bmatrix} \begin{bmatrix} V_n \\ V_r \end{bmatrix} \dots\dots\dots (1)$$

Where the subscript n is used to denote generator nodes and the subscript r is used for the remaining nodes.

Expanding equation (1),

$$I_n = Y_{nn} V_n + Y_{nr} V_r, \quad 0 = Y_{rn} V_n + Y_{rr} V_r$$

From which we eliminate V_r to find

$$I_n = (Y_{nn} - Y_{nr} Y_{rr}^{-1} Y_{rn}) V_n \dots\dots\dots (2)$$

Thus the desired reduced matrix can be written as follows,

$$Y_R = (Y_{nn} - Y_{nr} Y_{rr}^{-1} Y_{rn}) \dots\dots\dots (3)$$

It has dimensions (n x n) where n is the number of generators. Note that the network reduction illustrated by Eqs. (1) - (3) is a convenient analytical technique that can be used only when the loads are treated as constant impedances.

For the power system under study, the reduced matrices are calculated. Appendix II gives the resultant matrices before, during and after fault.

The power into the network at node i, which is the electrical power output of machine i, is given by [28].

$$P_{ei} = E_i^2 G_{ii} + \sum_{j=1}^n E_i E_j Y_{ij} \cos(\theta_{ij} - \delta_i + \delta_j) \quad i = 1, 2, 3, \dots, n \quad \dots(4)$$

Where,

$$\bar{Y}_{ij} = Y_{ij} \angle \theta_{ij} = G_{ij} + jB_{ij}$$

= negative of the transfer admittance between nodes i and j

$$\bar{Y}_{ii} = Y_{ii} \angle \theta_i = G_{ii} + jB_{ii}$$

= driving point admittance of node i

The equations of motion are then given by

$$\frac{2H_i}{\omega_R} \frac{d\omega_i}{dt} + D_i \omega_i = P_{mi} - \left[E_i^2 G_{ii} + \sum_{j=1}^n E_i E_j Y_{ij} \cos(\theta_{ij} - \delta_i + \delta_j) \right] \quad \dots(5)$$

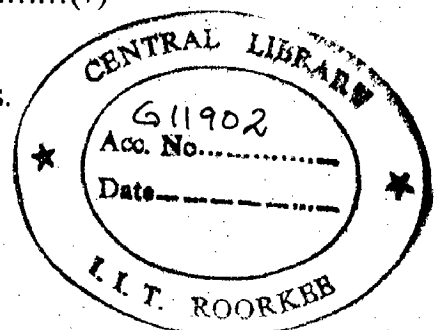
$$\text{and} \quad \frac{d\delta_i}{dt} = \omega_i - \omega_R \quad i = 1, 2, \dots, n \quad \dots(6)$$

It should be noted that prior to the disturbance (t = 0) $P_{mi0} = P_{ei0}$;

Thereby,

$$P_{mi0} = E_i^2 G_{ii0} + \sum_{j=1}^n E_i E_j Y_{ij0} \cos(\theta_{ij0} - \delta_{i0} + \delta_{j0}) \quad \dots(7)$$

The subscript 0 is used to indicate the pre-transient conditions.



As the network changes due to switching during the fault, the corresponding values will be used in above equations.

5.3.2 Simulink Models:

In this Dissertation work two types of model are used:

A. Classical Model.

B. Detailed model of Multimachine System with PSS.

A. Classical Model:

The classical model of a synchronous machine may be used to study the stability of a power system for a period of time during which the system dynamic response is dependent largely on the stored kinetic energy in the rotating masses. The classical model is the system this time on the order of one second or less. The classical model is the simplest model used in studies of power system dynamics and requires a minimum amount of data; hence, such studies can be conducted in a relatively short time and at minimum cost. Furthermore, these studies can be providing useful information. For example, they may be used as preliminary studies to identify problem areas that require further study with more detailed modeling. Thus a large number of cases for which the system exhibits a definitely stable dynamic response to the disturbances under study are eliminated from further consideration.

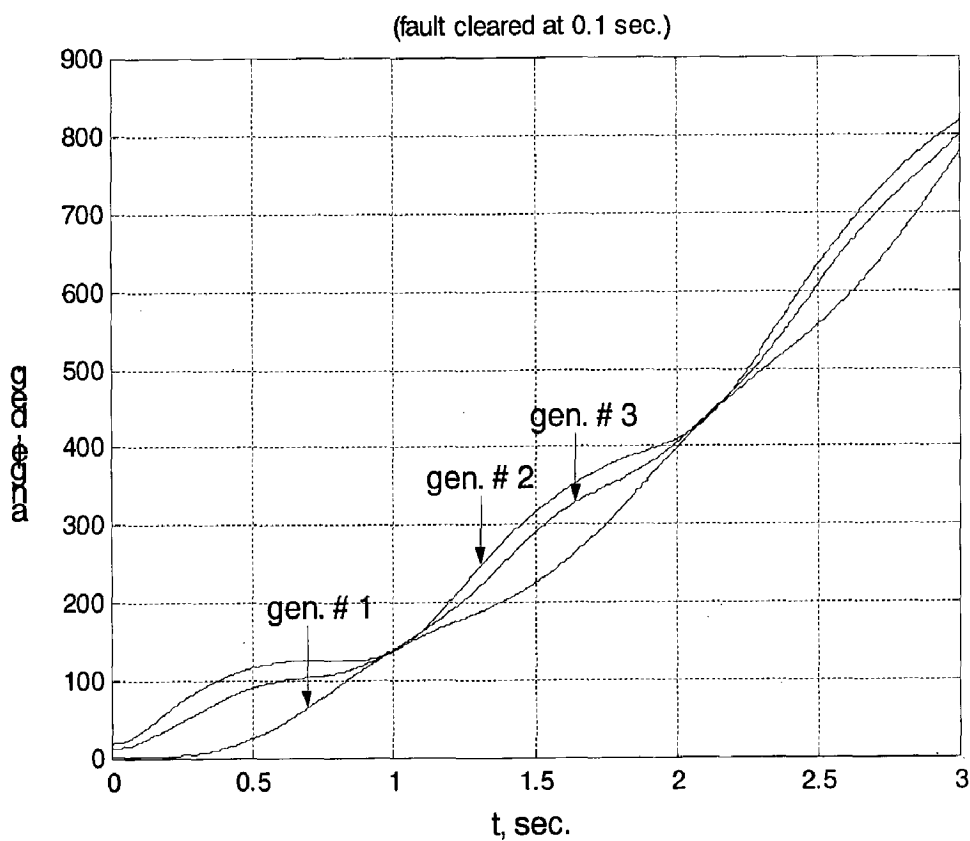
A classical study will be presented here on a small nine-bus power system that has three generators and three loads. A one-line impedance diagram for the system is given in Fig.1 (In appendix 5.1).

5.4 Simulation Result

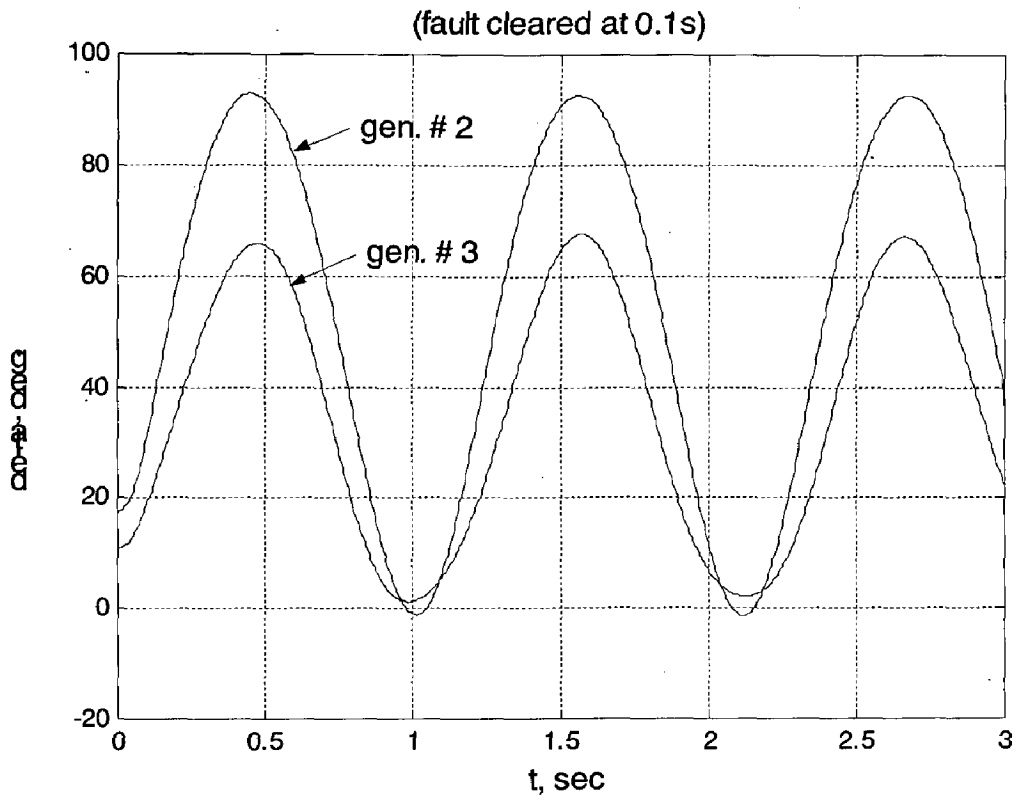
System responses are given for different values of fault clearing time (F.C.T.). Figures 1(a) and (b) show the individual generator angles and the difference angles (with gen. #1 as reference) for the system with F.C.T. = 0.1 sec., whereas Figs 1(c) and (d) show the rotor angular speed deviations and accelerating powers for the same case. The results show that the power system is stable in this case.

Figures 2.(a), (b) and (c) show the system responses for a F.C.T. value of 0.16 sec. At this point the system is critically stable. The system becomes unstable for F.C.T. = 0.17 sec., as the system responses in Figs 3.(a), (b) and (c) indicate.

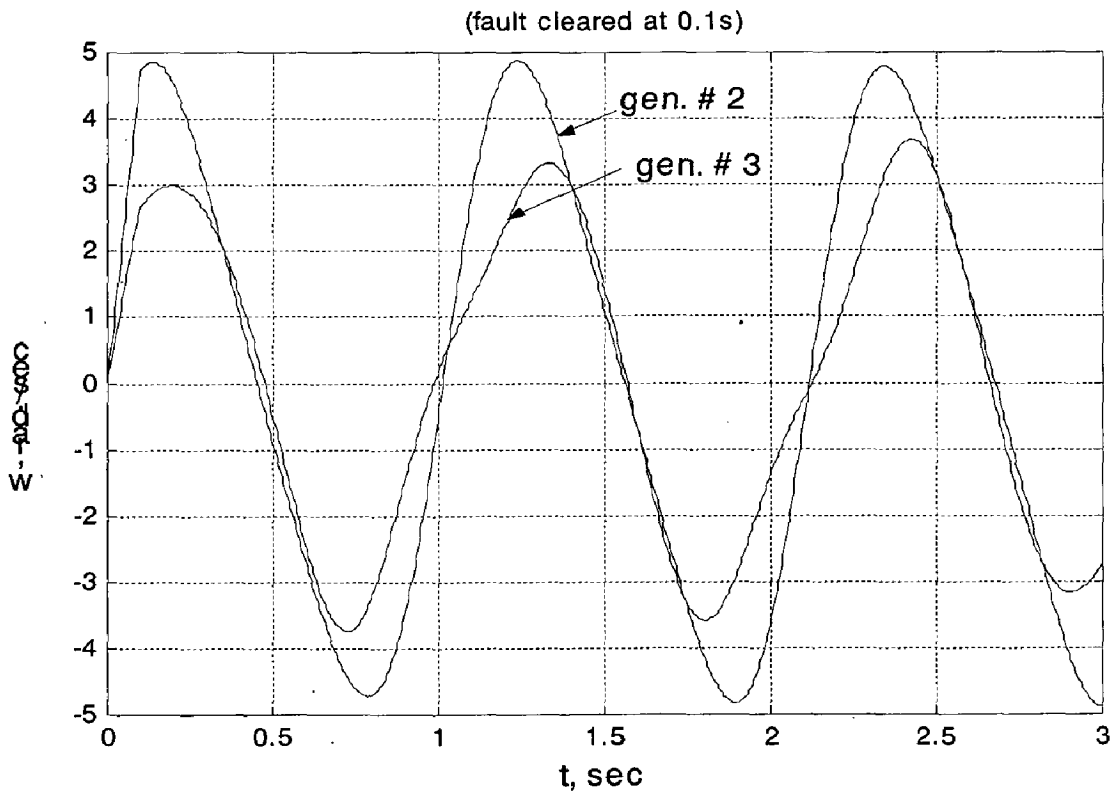
Thus a simple model based on Simulink, is very well suited for analyzing the transient stability performance of a power system under any system condition. The same model can also be extended to incorporate a more general (/practical) case of systems with exciters, turbines, speed governors etc.



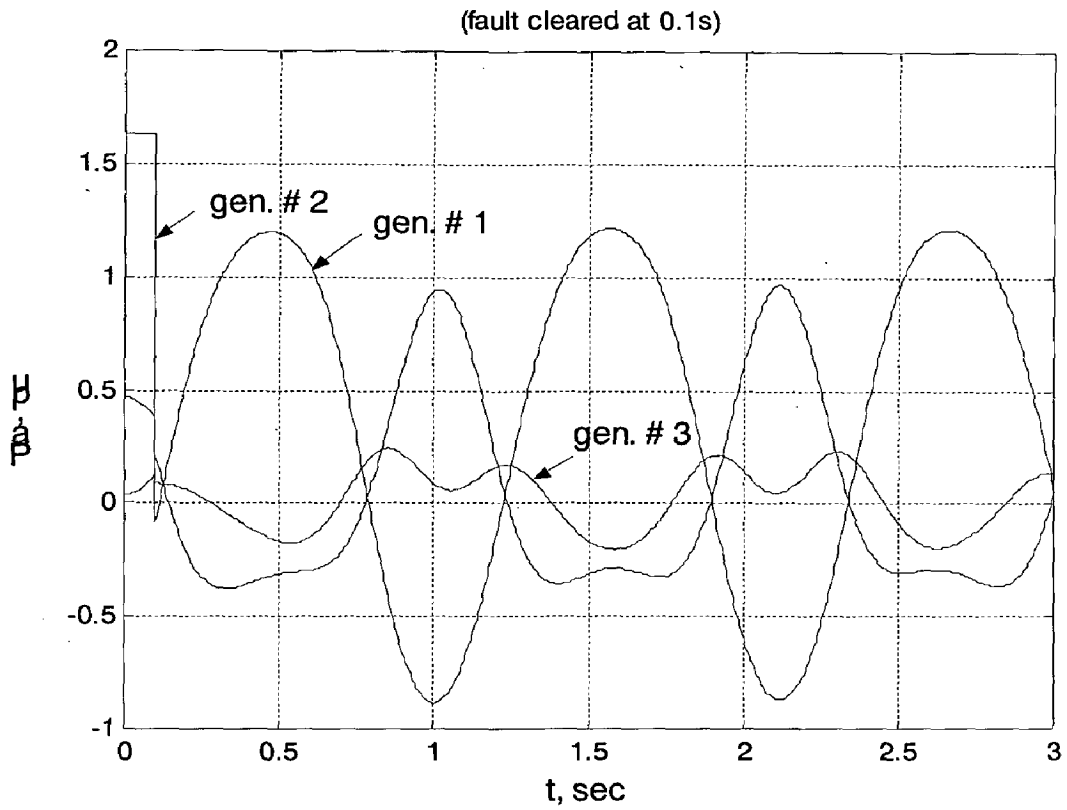
(a) Angular position of individual generators.



(b) Relative angular positions δ_{21} and δ_{31}

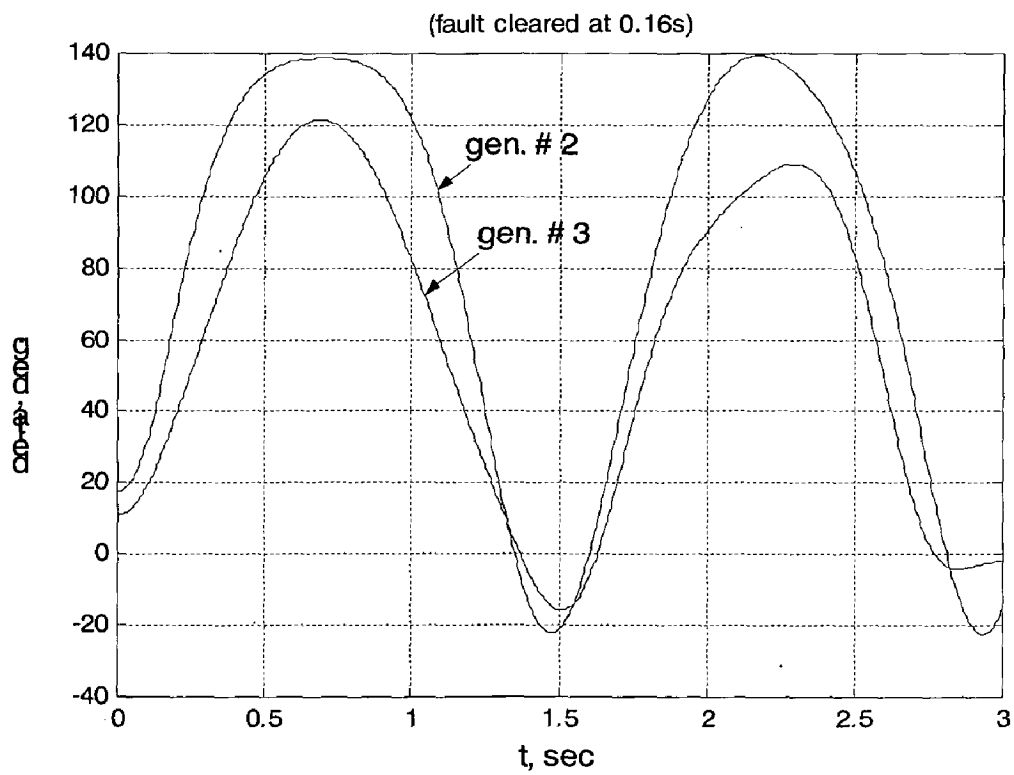


(c) Relative angular velocities ω_{21} and ω_{31}

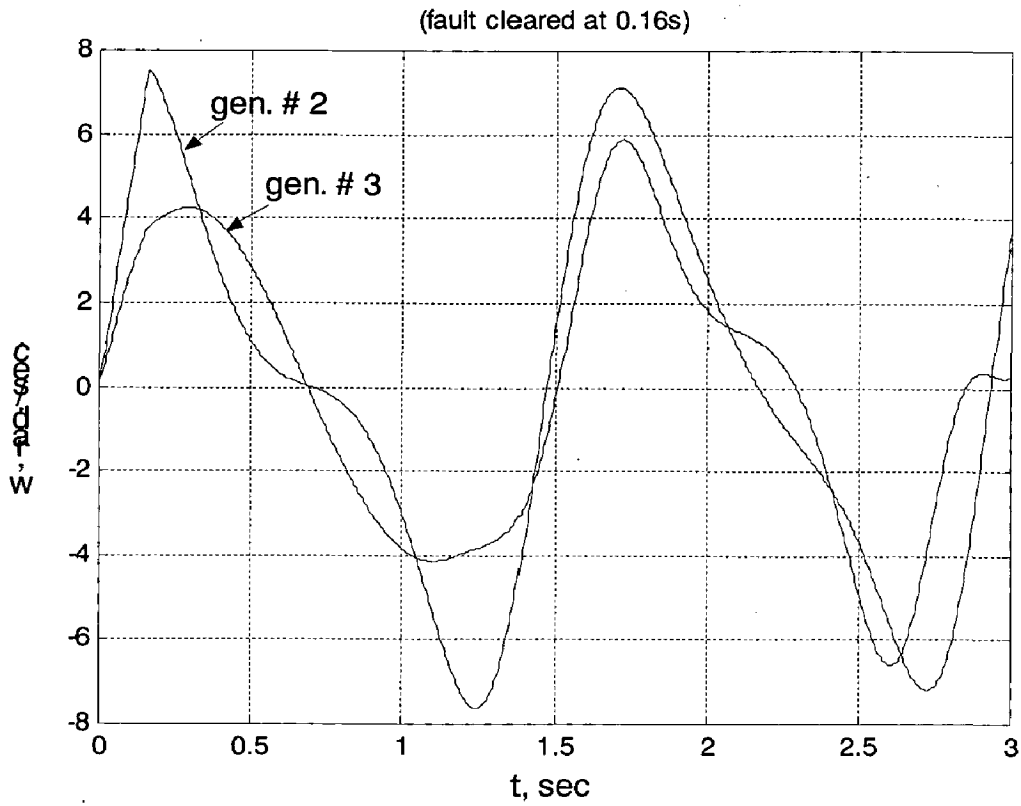


(d) Generator accelerating powers

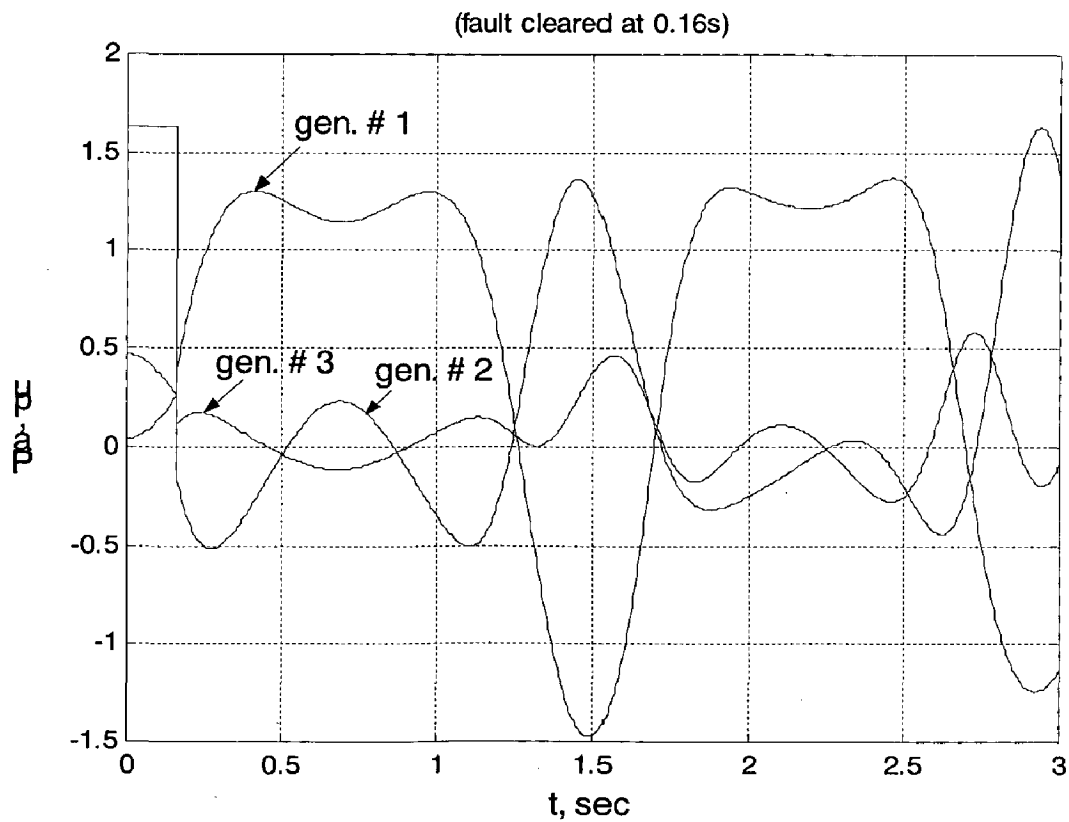
Fig. 5.1: System responses for F.C.T.= 0.1 sec.



(a) Relative angular positions δ_{21} and δ_{31}

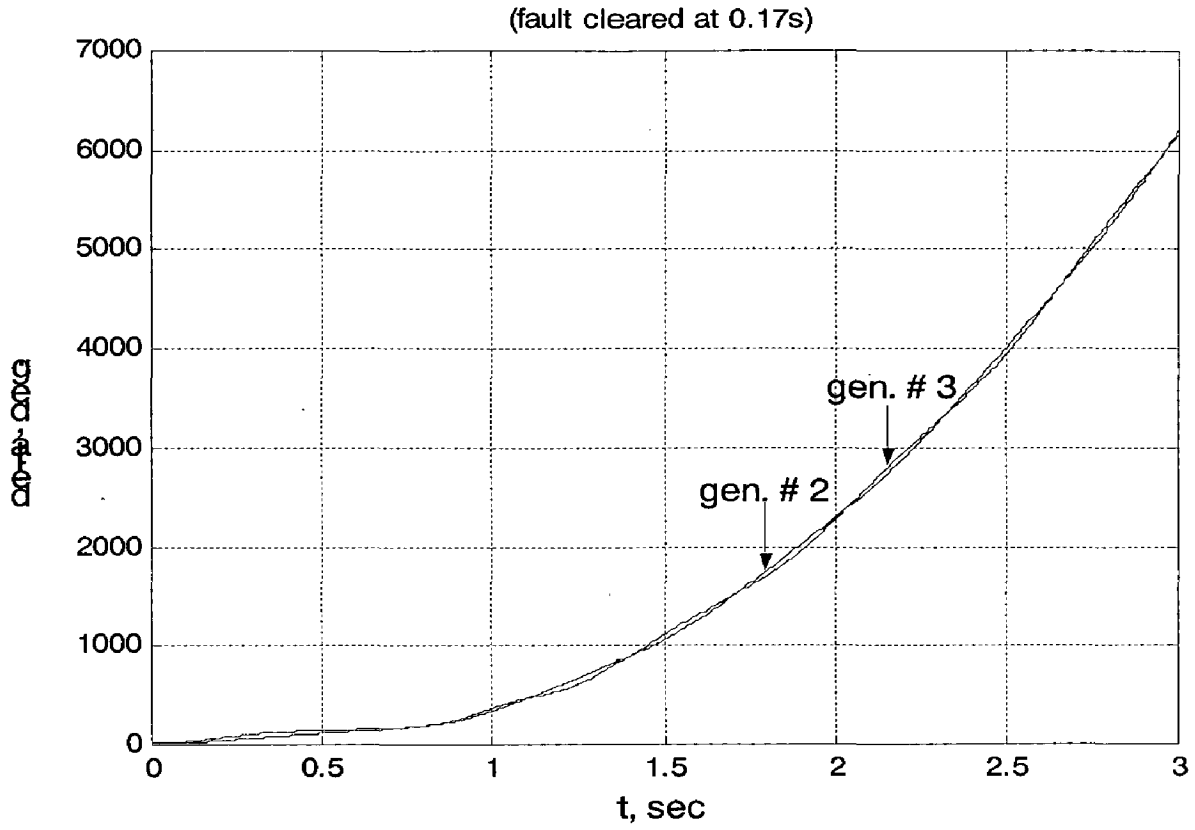


(b) Relative angular velocities ω_{21} and ω_{31}

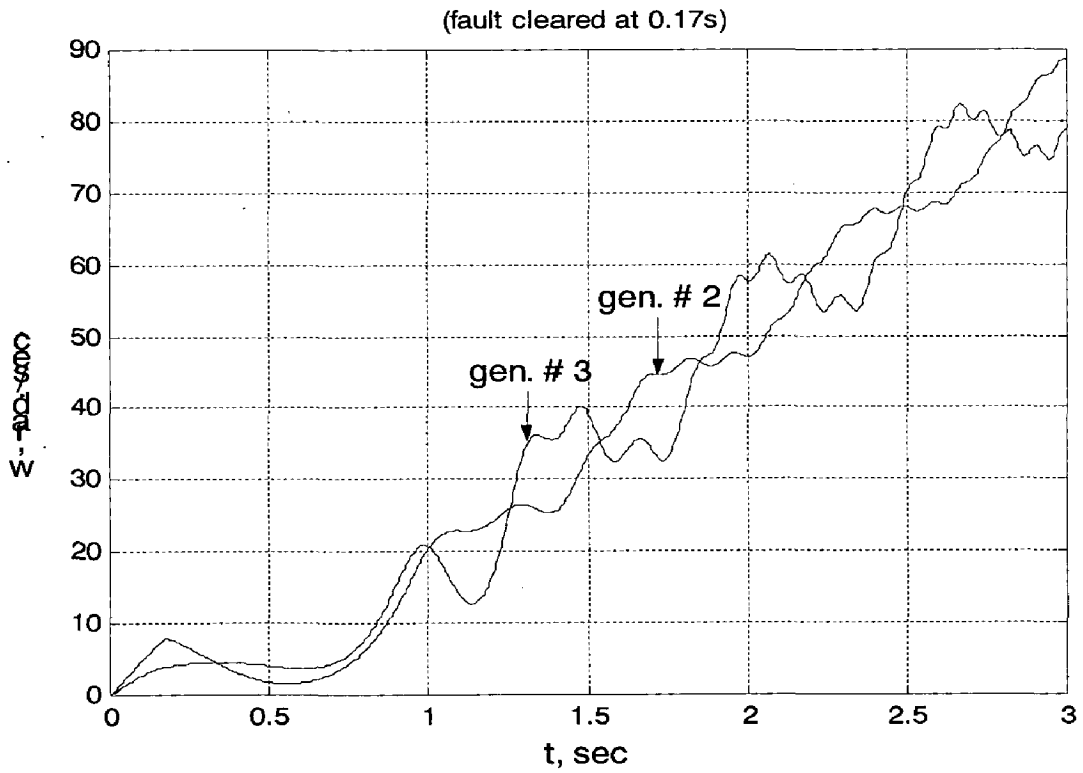


(c) Generator accelerating powers

Fig. 5.2: System responses for F.C.T.= 0.16 sec.



(a) Relative angular positions δ_{21} and δ_{31}



(b) Relative angular velocities ω_{21} and ω_{31}

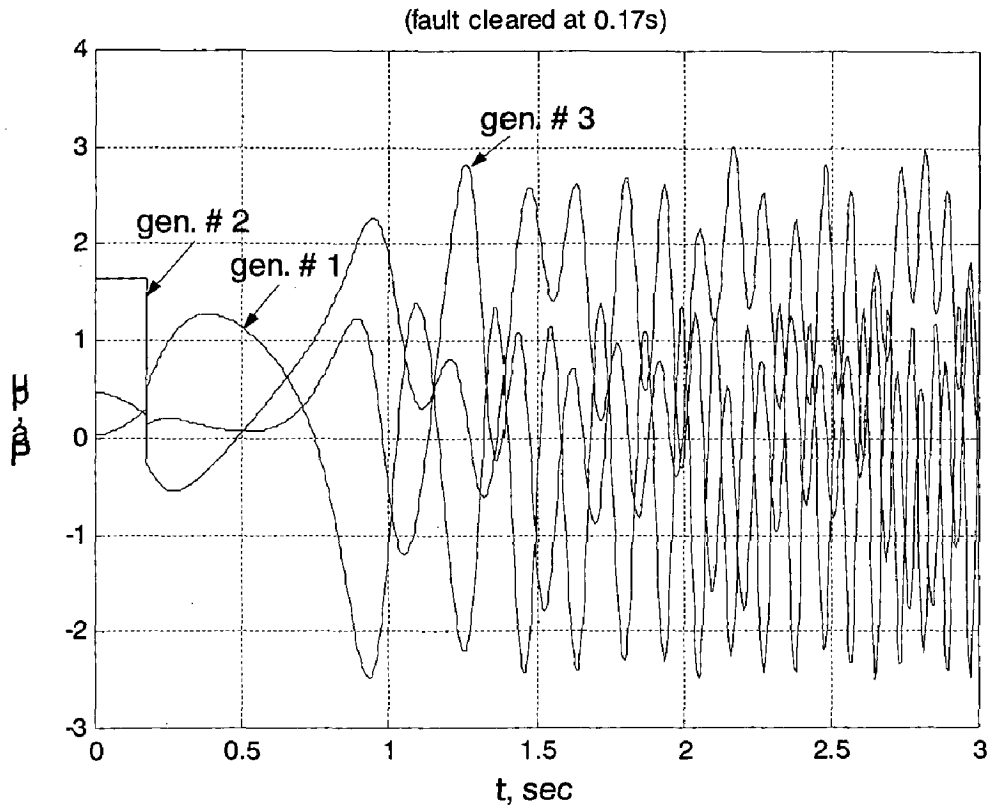
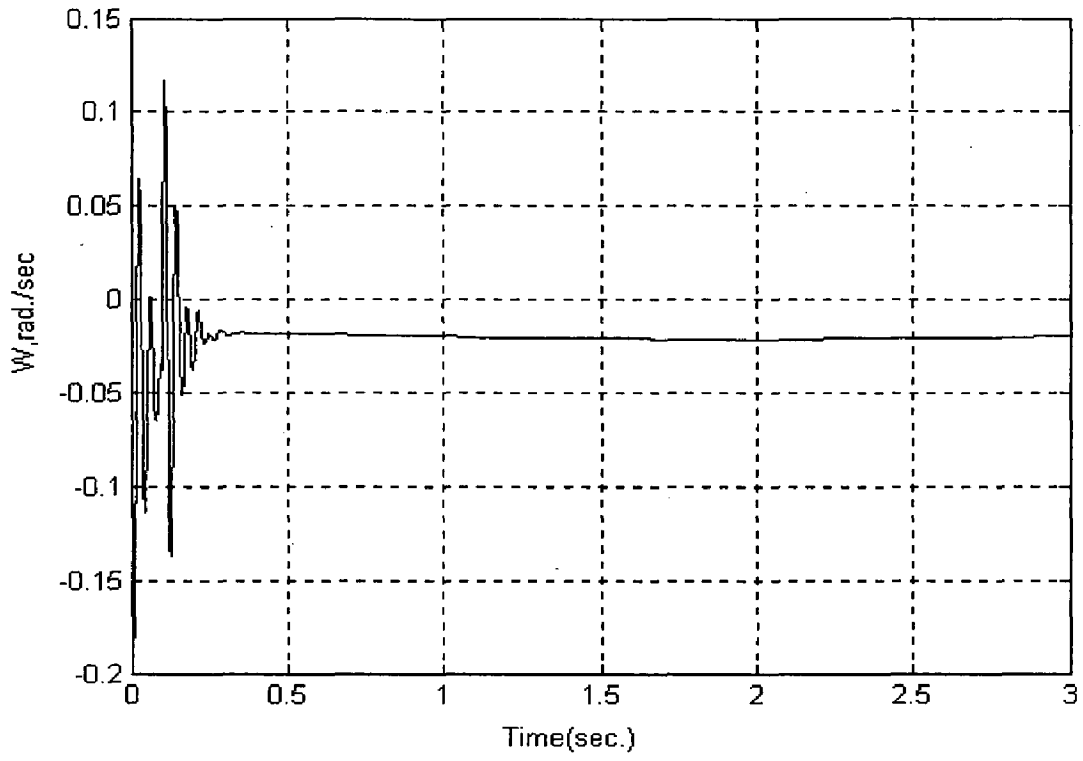


Fig. 5.3: System responses for F.C.T.= 0.17 sec

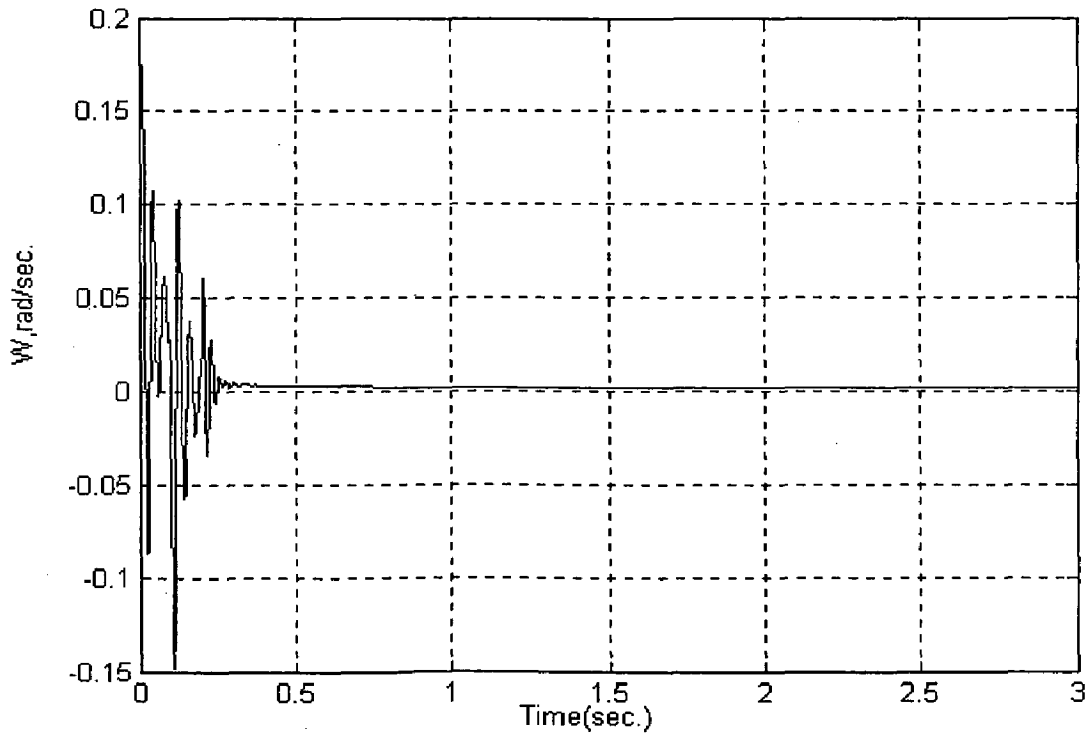
B. Detailed Model of Multimachine system with PSS

Thus a simple model based on Simulink, is very well suited for analyzing the transient stability performance of a power system under any system condition. The same model can also be extended to incorporate a more general (/practical) case of systems with exciters. So the detailed model of the multimachine system has the following simulation result:

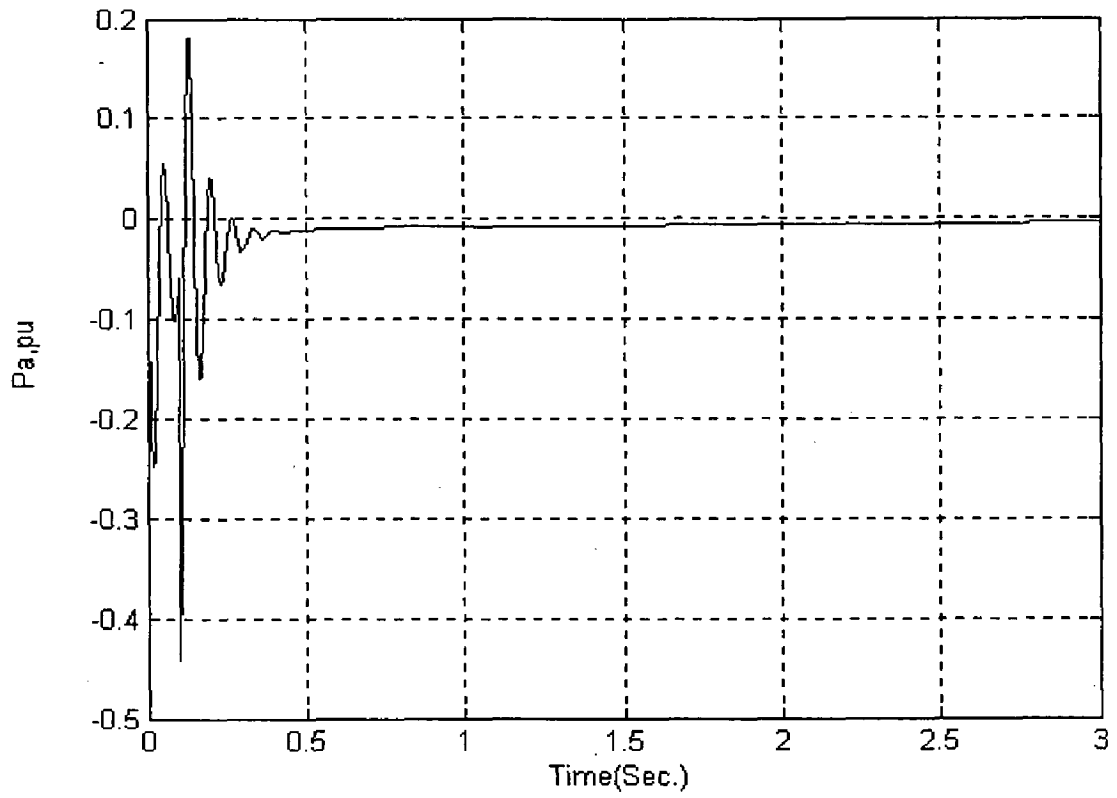
Case-1: When fault cleared at 0.1 sec



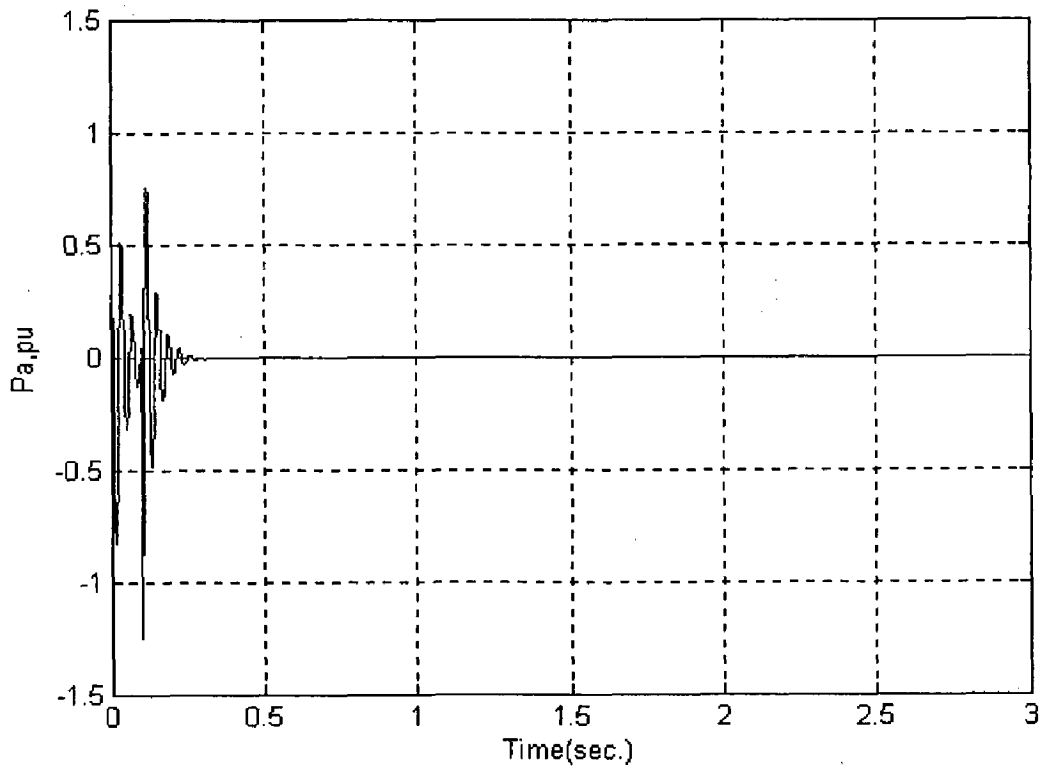
(a) Relative angular velocities ω_{21} .



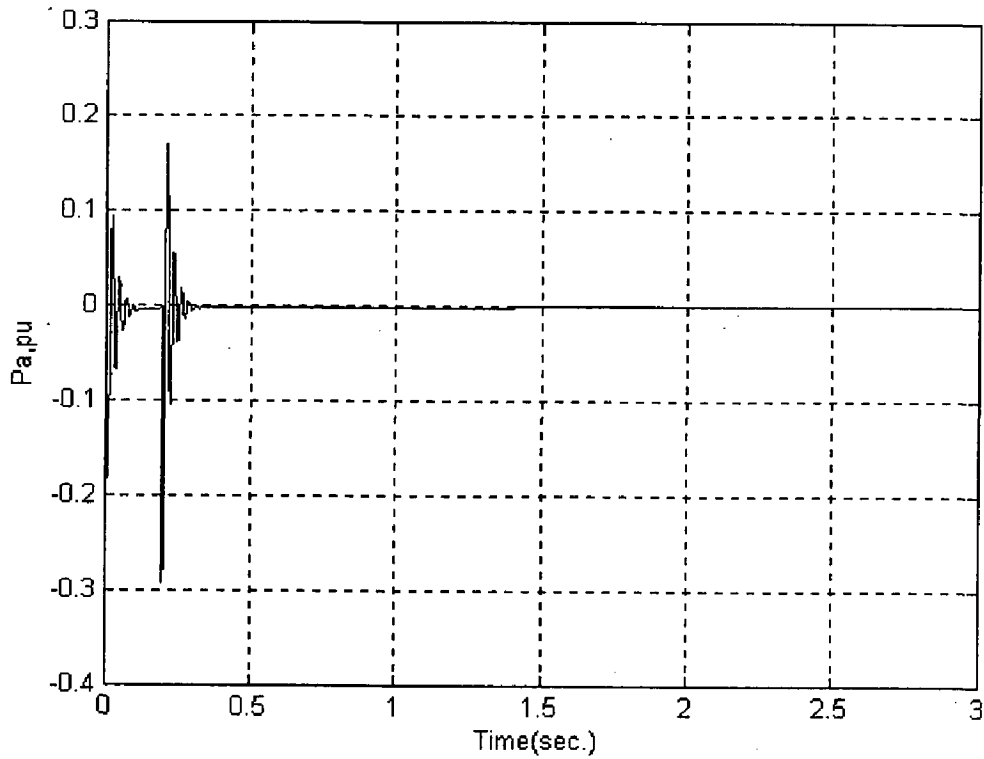
(b) Relative angular velocities ω_{23} .



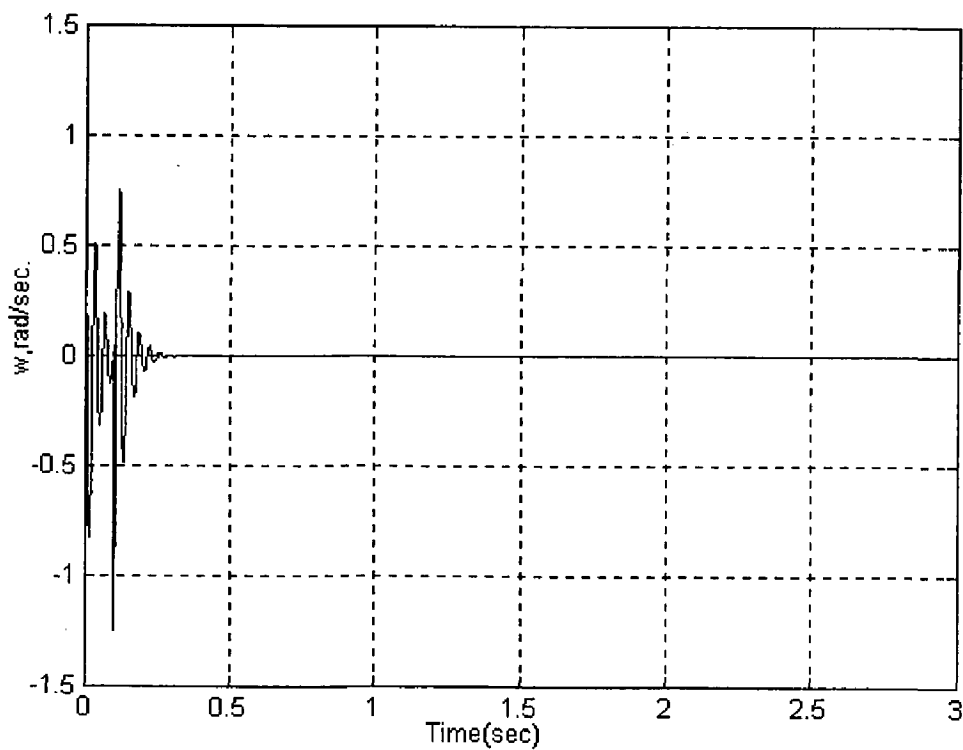
(c) Generator accelerating powers #1.



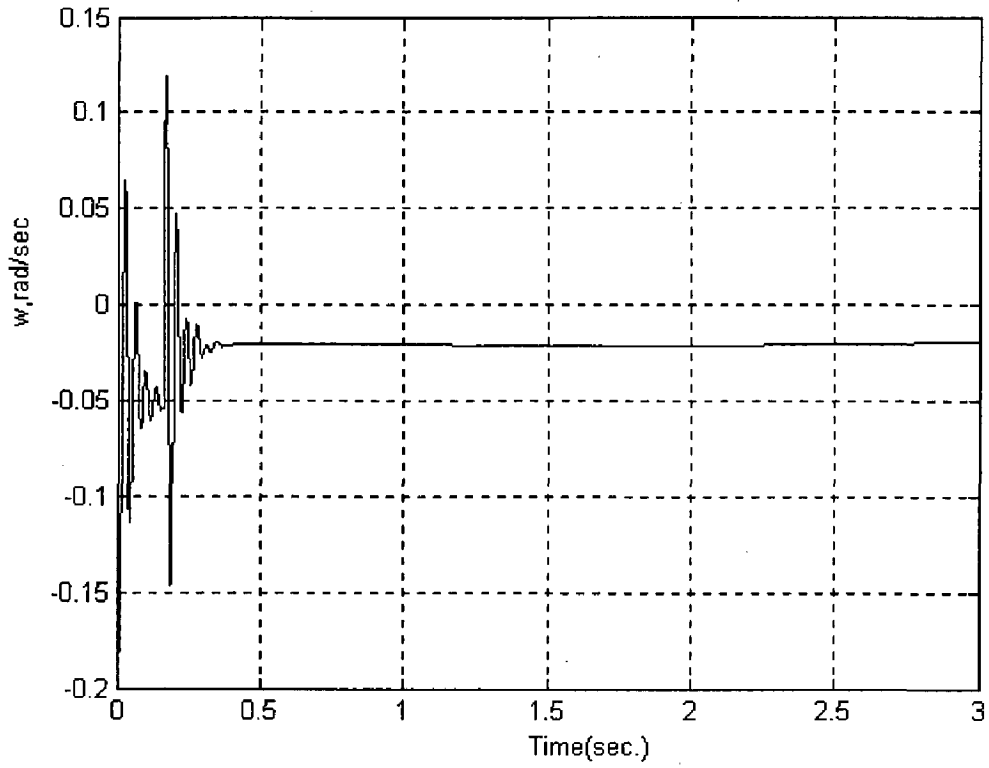
(d) Generator Accelerating Power #2.



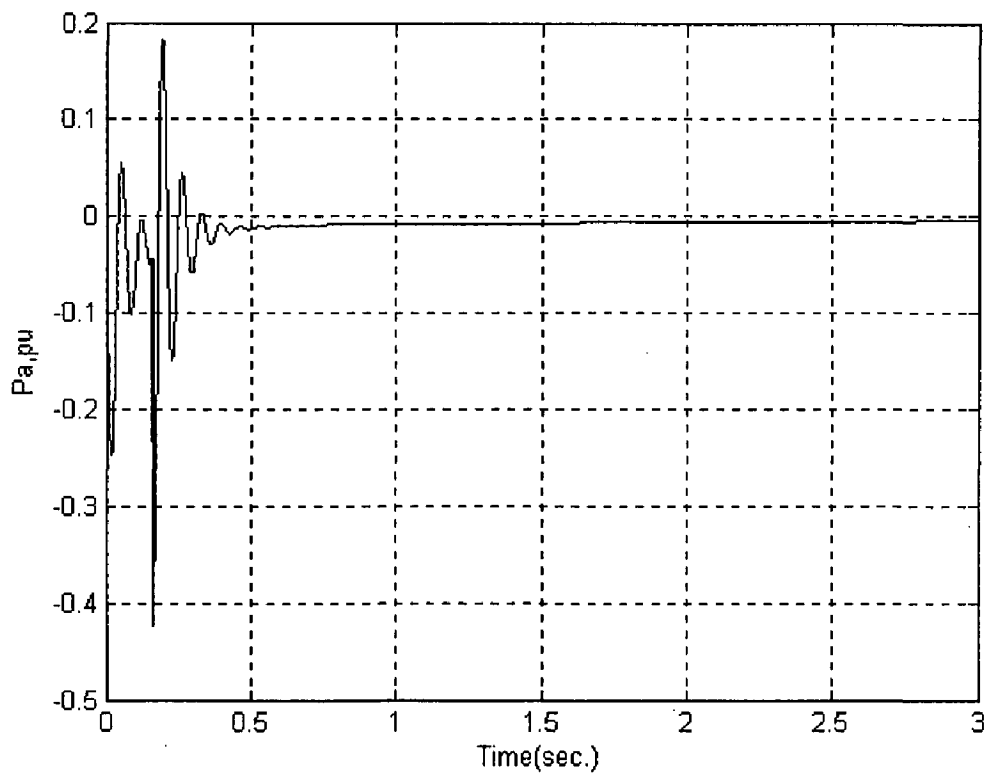
(e) Generator Accelerating Power #3.
 Fig.5.4: System responses for F.C.T.= 0.1 sec
 Case-2 when fault cleared at 0.16



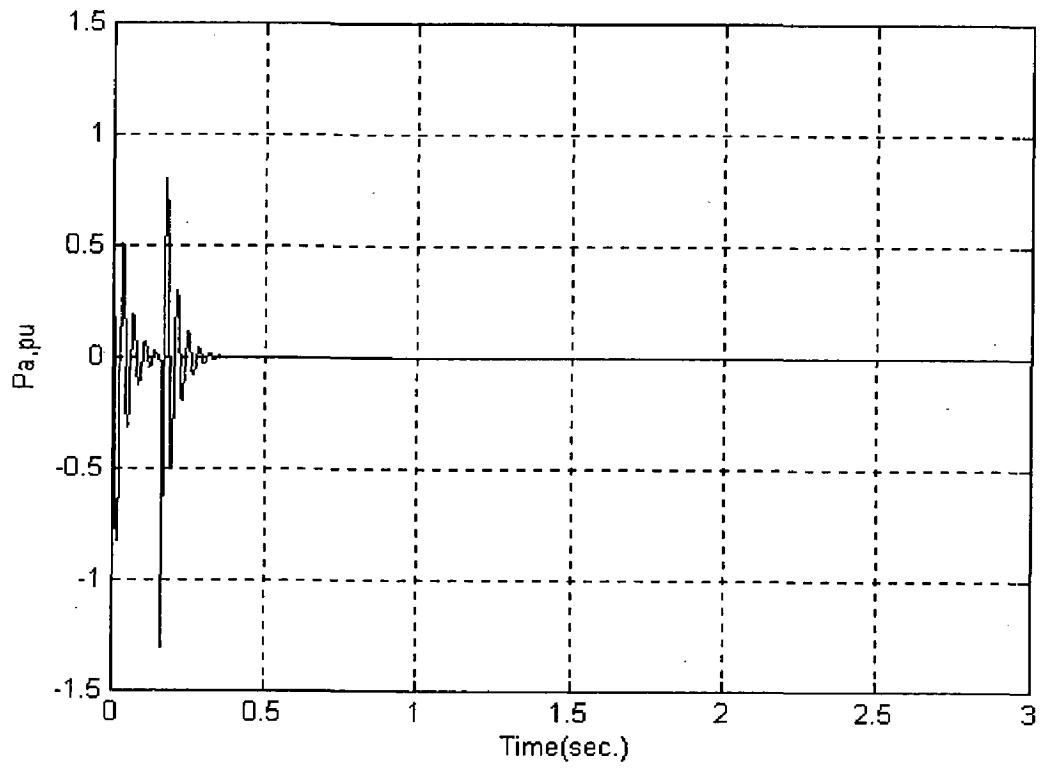
(a). Relative angular velocities ω_{21} .



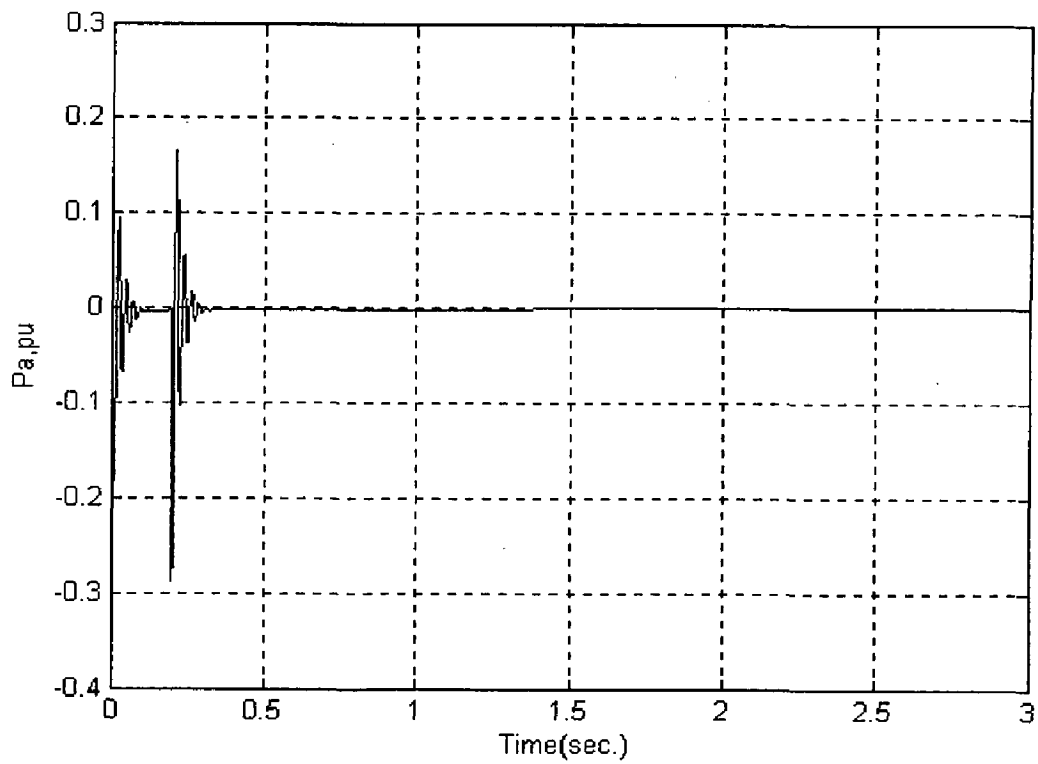
(b) Relative angular velocities ω_{23} .



(c) Generator accelerating power#1



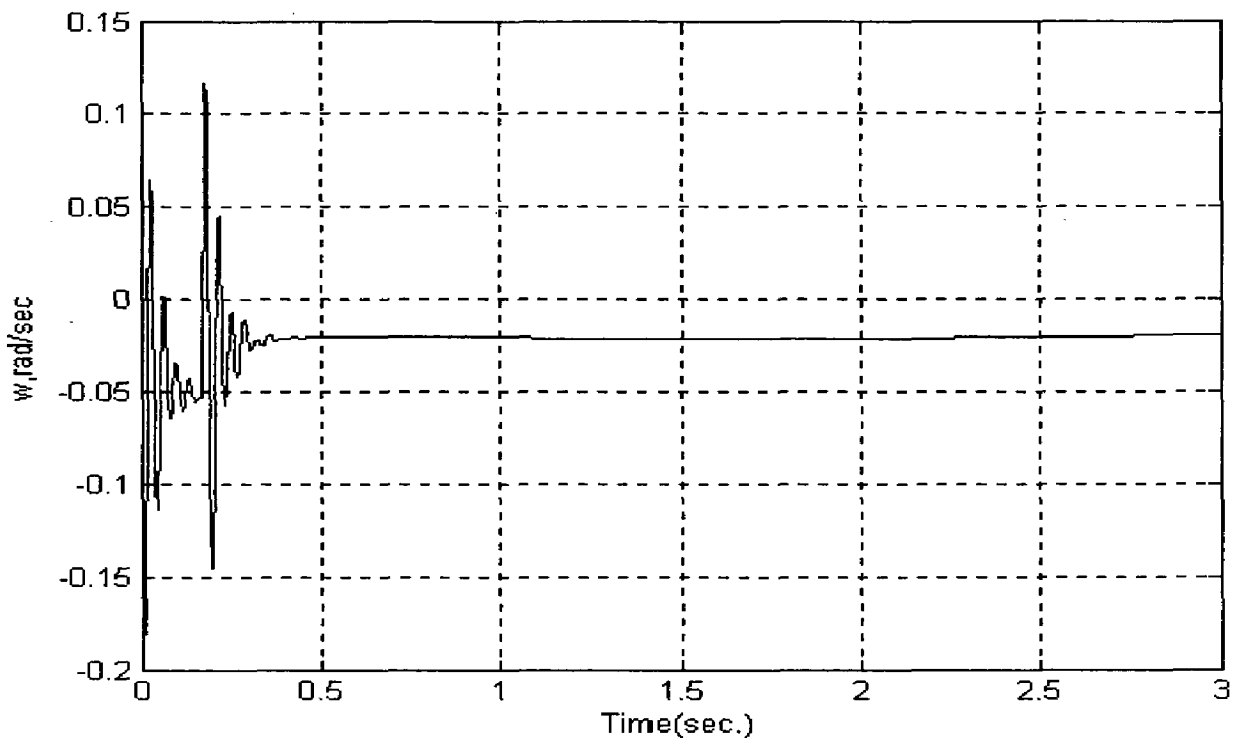
(d) Generator accelerating power #2



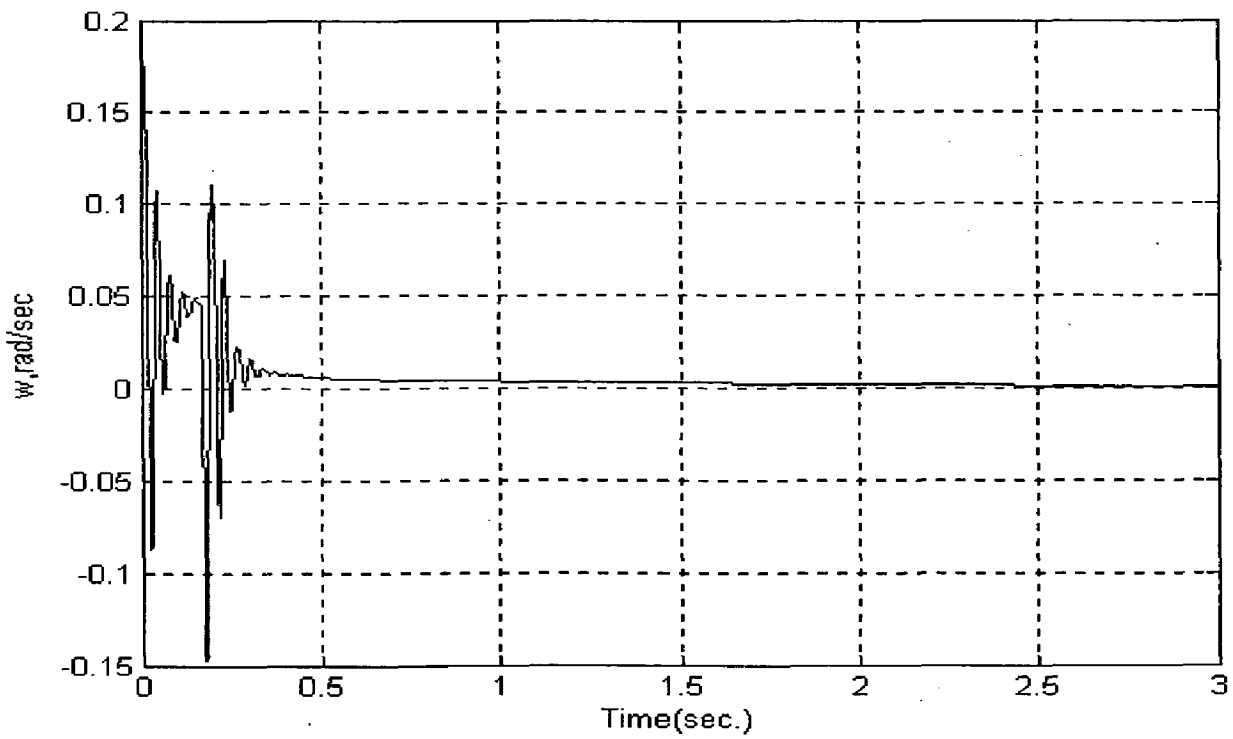
(e) Generator accelerating power #3

Fig.5.5: System responses for F.C.T.= 0.16 sec

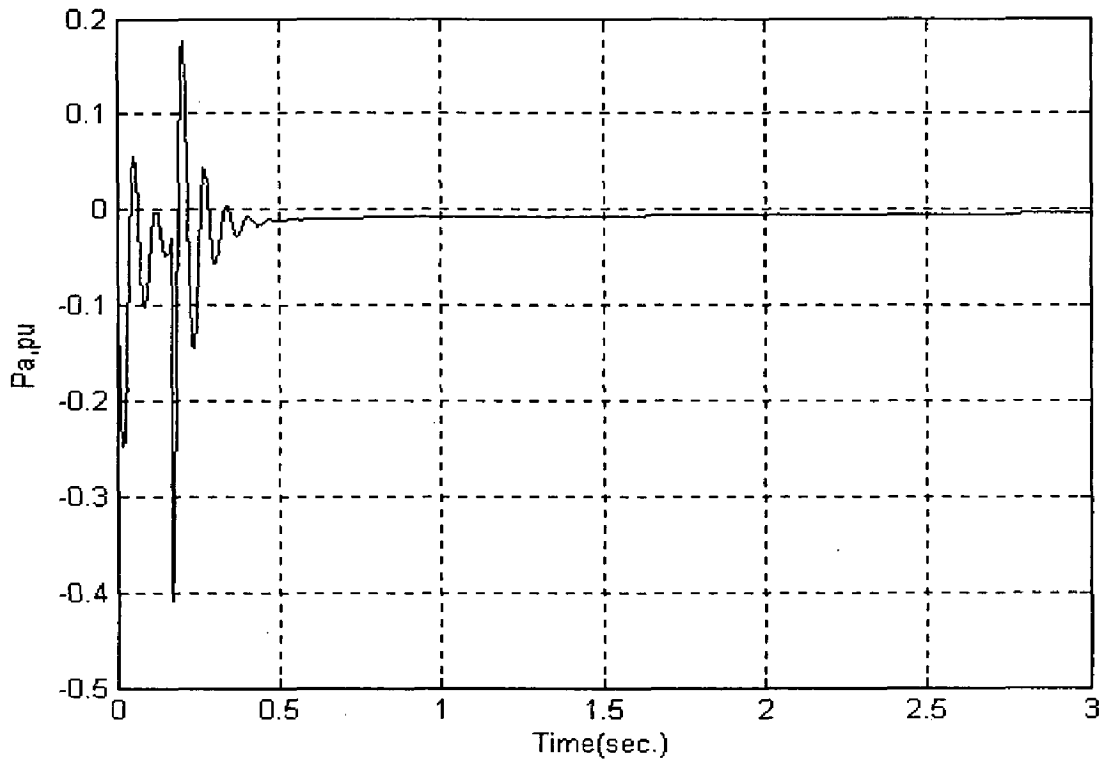
When fault cleared at 0.17;



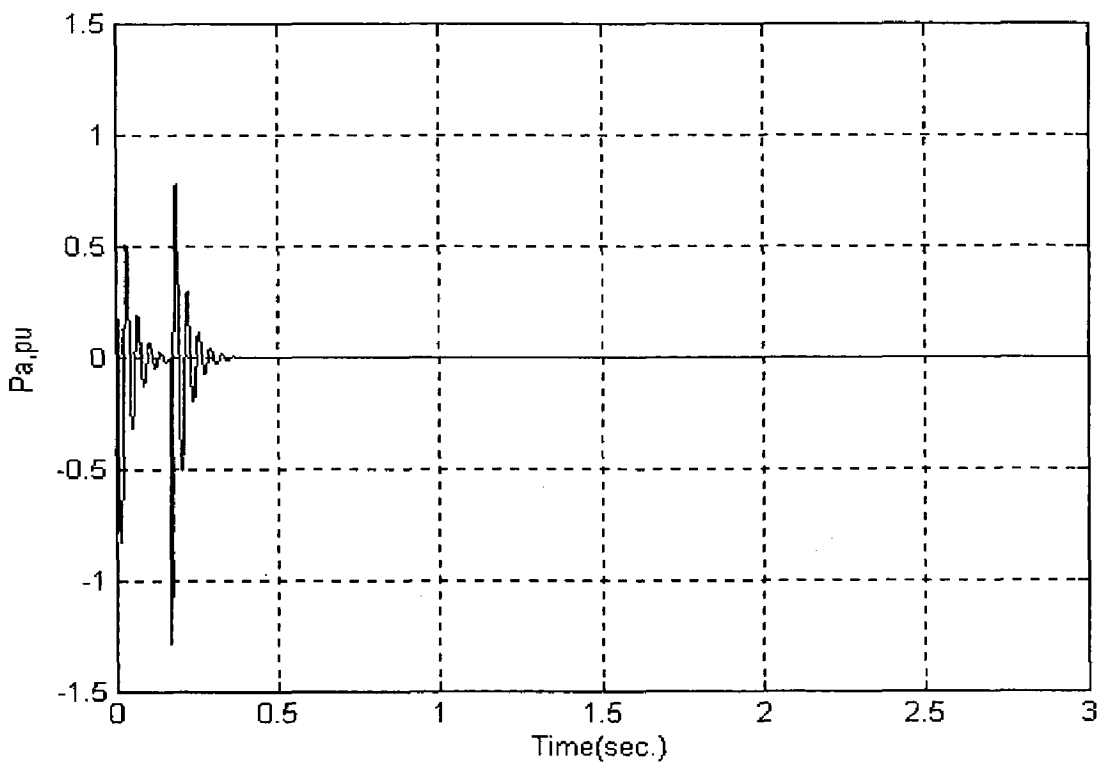
(a). Relative angular velocities ω_{21} .



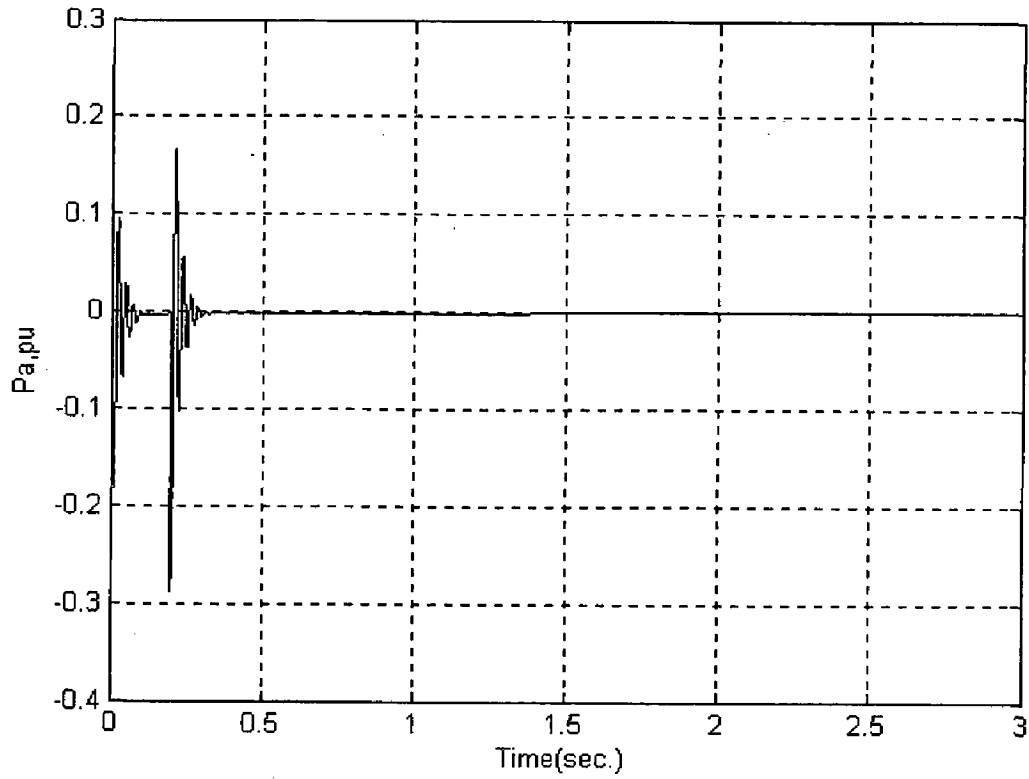
(b) Relative angular velocities ω_{23} .



(c). Generator Accelerating Power #1.



(d). Generator Accelerating Power #2.



(e). Generator Accelerating Power #3
Fig. 6.6: System responses for F.C.T.= 0.17 sec

6.1 Conclusion

6.1.1 The Following are the significant results of the investigated carried out for FLPSS

- Performance of an optimum conventional PSS is similar to that of FLPSS.
- Unsymmetrical triangular membership functions with $c_1 = 0.4$ provides the best dynamic performance of the FLPSS.
- The scaling factors decrease inversely with increase in magnitude of perturbation.
- FLPSS using adaptive scaling factors provide good performance

6.1.2 The Following are the significant results of the investigated carried out for Delta-Omega PSS

- Small perturbation model of SMIB system in state space form, with and without PSS has been developed.
- Studies show that parameter K_5 plays very important role in determining the small signal stability of the system. If K_5 is negative, increase in value of AVR gain adversely affects the small signal stability.
- A systematic approach has been introduced to tune the Delta-Omega PSS using frequency domain techniques.
- A detailed sensitivity analysis shows that the system dynamic responses are quite insensitive to wide variations in system loading conditions and parameter variations.

6.1.3 Identification of optimum locations for PSS for 3machine 9-bus system using Sensitivity and Participation methods is presented.

6.1.4 A new approach for tuning PSS of a multimachine system is

Proposed and tested for 3machine 9-bus system.

6.2 Scope For Future Work

- Investigation on Nero-Fuzzy PSS needs to be carried out.
- Fuzzy Logic PSS for a large multimachine system need to be explored.
- Effect of different Deffuzification Techniques like COG, COS, MOM, LOM and Bisector etc.
- Delta-Omega PSS for multimachine system.

13. Hiyama T., "Coherency-based identification of optimum site for stabilizer application", IEE.Proc, part c, V-130 part2, 1983.
14. Lim C.M. and Elangovan, S, "A new stabilizer design technique for multimachine power system", IEEE Trans. On Power Apparatus and Systems, PAS104, 1985.
15. HSU Y.Y. and Chen.C.L. "Identification of optimum location for power system stabilizer applications using participation factors", *ibid.*,134, 1987.
16. E.Z.Zhout, O.P.Malik, G.S.Hope, "Theory and Method of Power System Stabilizer Location". IEEE Trans. On Energy conversion, Vol. 6, No. 1, March 1991.
17. Chern-Lin Chen, Yuan-Yih Hsu, "An Efficient Algorithm For The Design Of Decentralized Out Put Feedback", IEEE Trans. On Power Systems, Vol.3, No.3, August 1998.
18. HSU Y.Y and Chen., C.L., " Identification of optimum location for power system stabilizer application using Participation factors". *IBID.*,134, 1987.
19. Y.Y. Hsu, C.H. Cheng, "Design of Fuzzy Power System Stabilizer for multimachine power system". IEE processing Vol.137 Part c, No.3 May 1990,pp 233-238.
20. Y.Y. Hsu, C.H. Cheng, "A Fuzzy Controller for Generation Excitation Control". IEEE transactions on Systems, Man, and Cybernetics, Vol. 23, No. 2, March/April 1993,pp 639-645.
21. M.A.M. Hassan, O.P.Malik and G.S.Hope, "A Fuzzy Logic Based Stabilizer for a Synchronous Machine." IEEE Transactions on Energy Conversion, Vol.6, No.3. September 1991, pp 407-413.
22. John M.Undrill, "Dynamic stability calculations for an arbitray number of inter connected machines", IEEE Trans. On Power Appratus and System, PAS-87, 1968.
23. Arcidiacono, V., Ferrari,E.,Marconanto,r., Dosghali,J. and Grandez,D.,"Evaluation and Improvement of electro-mechanical oscillation damping by means.
24. Eigenvalue-eigenvector analysis. Practical result in the Central Peru power system." IEEE Trans. On Power Apparatus and System,PAS-99, 1980.

25. P.Kundur, M.Klein, G.J.Rogers and M.S.Zywno, "Application of power system stabilizers for enhancement of overall system stability", IEEE Trans. On Power Systems, Vol. 4, No. 2, May 1989, pp 614-626.
26. A.Murdoch and A.Venkatraman, R.A.Lawson, "Integral of Accelerating Power Type PSS, Part-I Theory, Design, and Tuning Methodology". IEEE Trans. On Energy conversion, Vol. 14 No 4, Dec 1999. pp. 1658-1663.
27. A.Murdoch and A.Venkatraman, R.A.Lawson, "Integral of Accelerating Power Type PSS, Part-II Theory, Design, and Tuning Methodology". IEEE Trans. On Energy conversion, Vol. 14 No 4, Dec 1999. pp. 1664-1672.
28. Ramnarayan Patel, T.S.Bhatti and D.P.Kothari, "MATLAB/Simulink Based Transient Stability Analysis of a Multimachine Power System". International conference of Electrical Engineering Education (IJEEE), Vol.39, No. 4, Oct 2002.

APPENDIX 3.1

ELEMENTS OF MATRIX A (WITHOUT PSS, WITH AVR ONLY)

$$\begin{pmatrix} a_{11} & a_{12} & a_{13} & 0 & 0 \\ a_{21} & 0 & 0 & 0 & 0 \\ 0 & a_{32} & a_{33} & a_{34} & 0 \\ 0 & 0 & 0 & a_{44} & a_{45} \\ 0 & a_{52} & a_{53} & 0 & a_{55} \end{pmatrix}$$

Where

$$a_{11} = -K_d / (2 * H);$$

$$a_{12} = -K_1 / (2 * H);$$

$$a_{13} = -K_2 / (2 * H);$$

$$a_{21} = w_0;$$

$$a_{32} = -K_4 * K_3 / T_3;$$

$$a_{33} = -1 / T_3;$$

$$a_{34} = K_3 / T_3;$$

$$a_{44} = -1 / T_a;$$

$$a_{45} = -K_a / T_a;$$

$$a_{52} = K_5 / T_r;$$

$$a_{53} = K_6 / T_r;$$

$$a_{55} = -1 / T_r;$$

PERTURBATION MATRIX Γ

$$\begin{pmatrix} 1 / (2 * H) & 0 \\ 0 & 0 \\ 0 & 0 \\ 0 & K_a / T_a \\ 0 & 0 \end{pmatrix}$$

APPENDIX 3.2

The nominal parameters of the system investigated are following:

$$E_t = 1.0$$

$$H = 3.5 \text{ MJ/MVA}$$

$$R_e = 0$$

$$X_d = 1.81$$

$$X_q = 1.76$$

$$X_d' = 0.3$$

$$X_l = 0.16$$

$$D = 0$$

$$\Psi T_l = 0.2$$

$$R_a = 0.003$$

$$T_{do}' = 8.0 \text{ seconds}$$

$$A_{sat} = 0.031$$

$$B_{sat} = 6.9$$

$$K_a = 50$$

$$T_r = 0.02 \text{ seconds}$$

DEFINITION OF PARAMETERS K1-K6

$$K1 = \left. \frac{\Delta Te}{\Delta \delta} \right|_{\Delta \Psi_{fd}}$$

- Change in electric torque for a change in rotor angle with constant flux linkage in d-axis

$$K2 = \left. \frac{\Delta Te}{\Delta \Psi_{fd}} \right|_{\Delta \delta}$$

- Change in electric torque for a change in d-axis flux linkage with constant rotor angle.

$$K3 = \frac{X_{d'} + X_e}{X_d + X_e}$$

- Impedance factor

$$K4 = \frac{1}{K3} \frac{\Delta \Psi_{fd}}{\Delta \delta}$$

- Demagnetizing effect of a change in rotor angle.

$$K5 = \left. \frac{\Delta E_t}{\Delta \delta} \right|_{\Delta \Psi_{fd}}$$

- Change in generator terminal voltage for a change in d-axis flux linkage with constant rotor angle.

$$K6 = \left. \frac{\Delta E_t}{\Delta \Psi_{fd}} \right|_{\Delta \delta}$$

- Change in generator terminal voltage for a change in d-axis flux linkage with constant rotor angle.

$$efdo=ladu*ifdo;$$

$$\Psi_{ado} = xads*(-ido+ifdo);$$

$$\Psi_{aqo} = -xaqs*iqo;$$

$$\Psi_{ato} = \text{sqrt}(\Psi_{ado}^2 + \Psi_{aqo}^2);$$

$$ksdinc=1/(1+bsat*asat*\exp(bsat*(\Psi_{ato} - \Psi_{tl})));$$

$$ksqinc=ksdinc;$$

$$rt=ra+re;$$

$$xtq=xe+laqu*ksqinc+xl;$$

$$xdls=1/(1/(ladu*ksdinc)+(1/dfd));$$

$$xtd=xe+xdls+xl;$$

$$d=rt^2+xtq*xtd;$$

$$m1=eb*(xtq*\sin(\delta o)-rt*\cos(\delta o))/d;$$

$$n1=eb*(rt*\sin(\delta o)+xtd*\cos(\delta o))/d;$$

$$m2=xtq*ladu*ksdinc/(d*(ladu*ksdinc+dfd));$$

$$n2=rt*ladu*ksdinc/(d*(ladu*ksdinc+dfd));$$

$$k1=n1*(\Psi_{ado} + (laqu*ksqinc*ido))-m1*(\Psi_{aqo} + xdls*iqo);$$

$$k2=n2*(\Psi_{ado} + (laqu*ksqinc*ido))-m2*(\Psi_{aqo} + xdls*iqo)+xdls*iqo/dfd;$$

$$k3=dfd^2/(ladu*(dfd-xdls+m2*xdls*dfd));$$

$$k4=ladu*ladu*ksdinc*eb*(xtq*\sin(\delta o)-t*\cos(\delta o))/(d*(ladu*ksdinc+dfd));$$

$$k5=edo*(-ra*m1+x1*n1+laqu*ksqinc*n1)/et+eqo*(-ra*n1-x1*m1-xdls*m1)/et;$$

$$k6=edo*(-ra*m2+x1*m2+xdls*laqu*ksqinc*n2)/et+eqo*(-ra*n2-$$

$$x1*m2+xdls*((1/dfd)-m2))/et;$$

APPENDIX 3.5

ELEMENTS OF STSTE MATRIX A (WITH DELTA-OMEGA PSS)

$$\begin{pmatrix} a_{11} & a_{12} & a_{13} & 0 & 0 & 0 & 0 & 0 \\ a_{21} & 0 & 0 & 0 & 0 & 0 & 0 & 0 \\ 0 & a_{32} & a_{33} & a_{34} & 0 & 0 & 0 & 0 \\ 0 & 0 & 0 & a_{44} & a_{45} & a_{46} & 0 & 0 \\ 0 & a_{52} & a_{53} & 0 & a_{55} & 0 & 0 & 0 \\ a_{61} & a_{62} & a_{63} & 0 & 0 & a_{66} & a_{67} & a_{68} \\ a_{71} & a_{72} & a_{73} & 0 & 0 & 0 & a_{77} & a_{78} \\ a_{81} & a_{82} & a_{83} & 0 & 0 & 0 & 0 & a_{88} \end{pmatrix}$$

Where

$$a_{11} = -K_d / (2 \cdot H);$$

$$a_{12} = -K_1 / (2 \cdot H);$$

$$a_{13} = -K_2 / (2 \cdot H);$$

$$a_{21} = \omega_0;$$

$$a_{32} = -\omega_0 \cdot R_{fd} \cdot m_1 \cdot X_{dls};$$

$$a_{33} = -(\omega_0 \cdot R_{fd} / L_{fd}) \cdot (1 - (X_{dls} / L_{fd})) + m_2 \cdot X_{dls};$$

$$T_3 = -1 / a_{33};$$

$$a_{34} = K_3 / T_3;$$

$$a_{44} = -1 / a_{33};$$

$$a_{45} = -K_a / T_a;$$

$$a_{46} = K_a / T_a;$$

$$a_{52} = K_5 / T_r;$$

$$a_{53} = K_6 / T_r;$$

$$a_{55} = -1 / T_r;$$

$$a_{81} = K_{stab} \cdot a_{11};$$

$$a_{82} = a_{12} \cdot K_{stab};$$

APPENDIX-5.1

Generator Data

Generator No.	1	2	3
Rated MVA	247.5	192.0	128.0
kV	16.5	18.0	13.8
H(sec)	23.64	6.4	3.01
Power Factor	1.0	0.85	0.85
Type	Hydro	Steam	Steam
Speed	180r/min	3600r/min	3600r/min
x_d	0.1460	0.8958	1.3125
x_d	0.0608	0.1198	0.1813
x_q	0.0969	0.8645	1.2578
x_q	0.0969	0.1969	0.25
x_l (leakage)	0.0336	0.0521	0.0742
T_{do}	8.96	6.00	5.89
T'_{qo}	0	0.535	0.600
Stored energy at rated speed	2364MW.s	640MW.s	301MW.s

Note: Reactance values are in pu on a 100-MVA base. All time constants are in seconds.

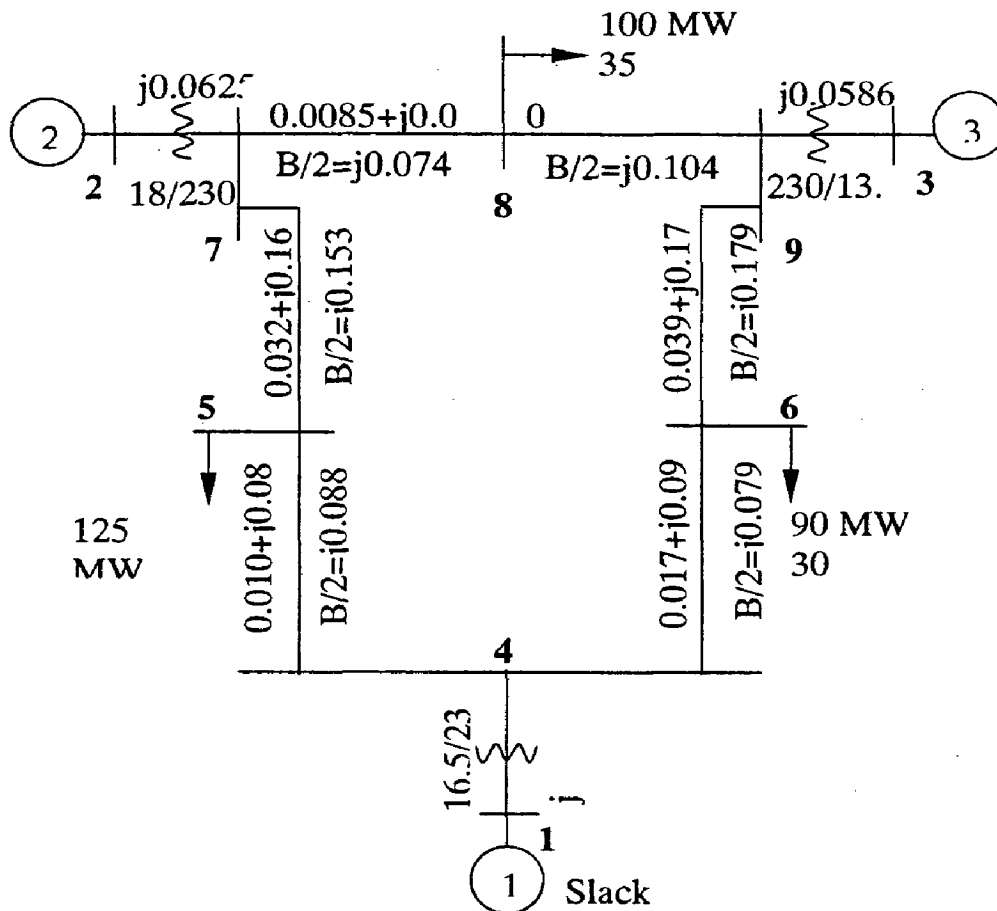


Fig. 1: WSCC 3-machine, 9-bus system; all impedances are in pu on a 100-MVA base

NOMENCLATURE

K_{sd} = saturation factor for direct axis inductance.

K_{sq} = saturation factor for quadrature axis inductance

K_{sd} (iner) = incremental saturation factor for direct axis inductance.

K_{sq} (iner) = incremental saturation factor for quadrature axis inductance.

R_e = line resistance.

X_e = line inductance.

R_a = armature resistance.

R_{fd}, L_{fd} = are respectively rotor circuit resistance and inductance.

E_{fd} = field voltage

Ψ_{fd} = Rotor circuit flux linkage.

I_d = direct axis component of current at the generator terminals.

I_q = quadrature axis component of current at the generator terminals.

T_e = air gap torque.

T_{do} = mechanical torque applied.

Ψ_{aq}, Ψ_{ad} = Flux linkages of the armature in the quadrature and direct axis respectively.

V_1 = voltage output across the transducer.

E_t = terminal voltage magnitude.

E_b = voltage at the infinite bus.

L_q, L_d = are stator self-inductances.

L_l = Linkage inductance.

L_{ad} and L_{aq} = are mutual component of L_d & L_q respectively.

L_{adu} = is the unsaturated value of L_{ad} and L_{ads} is the saturate value.

P = Generator real power output

Q = Generator reactive power output

S = Lap lace operator.

X = State vector

A = System Matrix

B = Control Matrix

p = Perturbation Matrix.

Δ = Small perturbation.

E_d = d-axis component of E_t .

E_q = q- axis component of E_t .

E_{bd} = d-axis component of E_t .

E_{bq} = q-axis component of E_b .

I_{fd} = generator field current.

I_t = generator field current.

f = system frequency.

H = Inertia Constant.

φ = Power factor angle between E_t & I_t .

δ_i = Load angle (angle between E_t and quadrature axis).

δ_o = Angle between infinite bus voltage and quadrature axis.

ω = Angular speed.

T_m = Mechanical Torque.

P_e = Air gap power.

T_e = Electrical Torque.

T_m = Mechanical Torque.

X_d = Direct axis reactance of synchronous machine.

X_q = Quadrature axis reactance of synchronous machine.

X_l = Leakage reactance of synchronous machine.

X_d' = Direct axis transient reactance of synchronous machine.

X_q' = Quadrature axis transient reactance of synchronous machine.

Ψ_{at} = Air gap or mutual flux linkage.

Ψ_{ad} = d-axis component of air gap flux linkage.

Ψ_{aq} = q-axis component of air gap flux linkage.

Ψ_{r1} = Machine saturation parameter.

A_{sat} = Constant depending upon saturation characteristic.

B_{sat} = Constant depending upon the saturation characteristic.

K_{sdinc} = Incremented saturation factor of direct axis.

K_{sd} = Saturation factor of quadrature axis.

K_{sqinc} = Incremental saturation factor of quadrature axis.

L_{ads} = Saturated value of direct axis mutual reactance of synchronous machine.

L_{aqu} = Unsaturated value of quadrature axis mutual reactance of synchronous machine.

T_{do}' = Direct axis transient open circuit time constant.

K_a = AVR gain.

V_s = Stabilizer signal.

V_{ref} = AVR reference signal.

K_{stab} = Stabilizer gain.

K_{s1}, K_{s2}, K_{s3} = Stabilizer parameters.

$T_w, T_{w1}, T_{w3}, T_{w3}, T_{w4}$ = Washout time constants of PSS.